DEVELOPMENT OF AN AUTOMATED DYNAMIC CONE PENETROMETER FOR EVALUATING SOILS AND PAVEMENT MATERIALS

Final Report
Project: FLDOT-ADCP-WPI #0510751

by
Frazier Parker
Mike Hammons
Jim Hall

Highway Research Center
Auburn University, Alabama

for
Florida Department of Transportation
Gainesville, Florida

July 1998

ACKNOWLEDGMENTS

This report was prepared by the Auburn University Highway Research Center and Applied Research Associates, Inc. in cooperation with the State of Florida Department of Transportation and the U. S. Department of Transportation. The opinions, findings and conclusions expressed in this publication are those of authors and not necessarily those of the Florida Department of Transportation.

ABSTRACT

The correlation between the resistance to the penetration of cone penetrometers has historically been used to estimate in situ soil and paving material strength. This report reviews the literature related to the use of dynamic cone penetrometers (DCP) for evaluating soil and paving material strength.

Manually driving the penetrometer, recording blows versus penetration, and extracting the device is a somewhat tedious process. Automation of this process means more efficient and cost effective data collection, and the design, fabrication and operation of an automated dynamic cone penetrometer (ADCP) is described.

Demonstration and calibration tests with the ADCP in typical Florida paving materials and subgrade soils were conducted. Analysis of the data from these tests demonstrates the strength of Florida paving materials and subgrade soils can be readily estimated with data from the ADCP and existing correlations. Additional research to establish relationships between laboratory/design strength parameters and field strength parameters estimated with the ADCP will be required to effectively utilize the ADCP for construction control.

TABLE OF CONTENTS

LIST OF TABLES

LIST OF FIGURES

INTRODUCTION

Background

There is a direct correlation between the strength of soil and paving materials and the resistance to their penetration by solid objects, in particular cone penetrometers. This correlation has historically been used to estimate in situ soil and paving material strength by measuring penetration resistance.

Fenwick (1) describes military applications of the airfield cone penetrometer and the trafficability cone for decisions regarding operations of aircraft and vehicles on unsurfaced soils. The devices are pushed by hand into the soil and the required force measured. This process limits the strength of soils and depths which can be evaluated. In addition, there can be considerable variability between operators and correlations with soil strength properties, such as CBR, are generally poor. Croney and Croney (2) report a hand held cone penetrometer used in England to check uniformity of subgrade construction and to indicate in situ CBR. Correlations are found reasonable for fine grained soils but not for granular soils.

Driving a device, i.e., dynamic cone penetrometer (DCP), alleviates many of the deficiencies of systems that are manually pushed into soil or paving materials. The device remains relatively simple in design and operation, but permits testing soils and paving materials with a full spectrum of strength to depths that are typically considered sufficient. Operator variability is reduced and correlations with strength parameters are more accurate.

The concept for currently used DCP's was originally formulated and developed in South Africa (3,4). The DCP consists of a steel rod with a cone at one end which is driven into the pavement structure and subgrade by means of a sliding hammer. Material strength is indicated by the penetration achieved (usually in millimeters) per hammer blow. The cone has an angle of 30 degrees with a diameter of 20 mm. The hammer mass is 8 kg with a drop height of 575 mm. The

version of the DCP adopted for automation contains several modifications proposed by researchers at the Waterways Experiment Station, Vicksburg, MS (5). Modifications, illustrated in Figure 1, include a cone angle of 60 degrees and the option to use a 4.6 kg hammer for weaker soils.

Automation

Operating the DCP, particularly extracting the cone, can be physically arduous and the collection and manipulation of data tedious and time consuming. These restrictions tend to limit testing that can be reasonably accomplished with the DCP and has lead to efforts to automate the operation, data collection and analysis procedures, i.e., the automated dynamic cone penetrometer (ADCP).

Livneh, Ishai and Livneh (6) describe an ADCP developed by the Israeli Institute of Technology. The ADCP consists of a pneumatic system for raising the DCP weight, a vertical frame with wheels for carrying the DCP hammer lifting and release mechanism and the penetration rod. The weight is lifted to the proper height by the pneumatic cylinders and released to fall freely at the prescribed drop height.

Ese, Myre, Noss and Vaerness (7) describe an ADCP fabricated in Norway. In the Norwegian design, the DCP is suspended by a chain mounted onto a wheel to insure a vertical orientation. The hammer is lifted by two pneumatic shuttle cylinders which follow as the rod penetrates into the subgrade. Penetration is measured by a rotary encoder on the chain wheel and sent to a PC. The pneumatic cylinders operate the hammer in reverse direction to remove the rod at completion of a test.

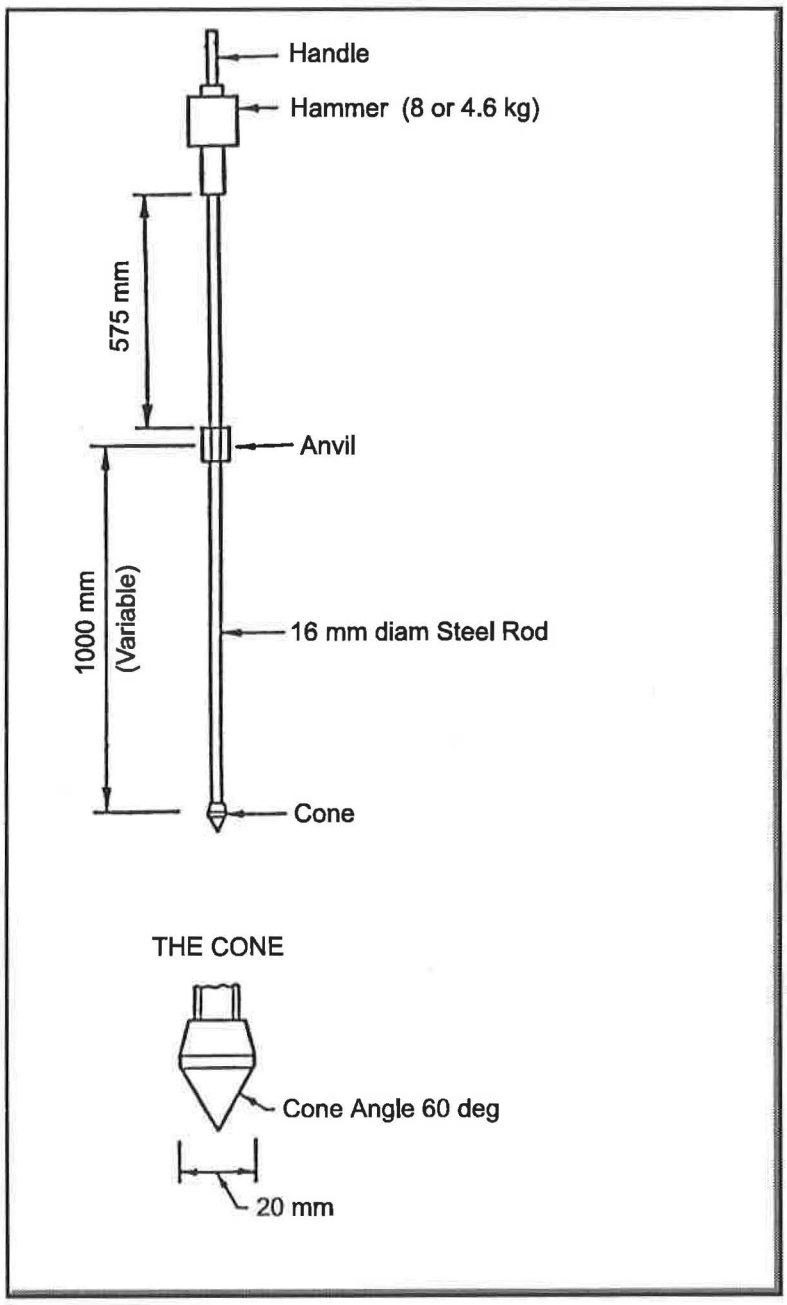

Figure 1. Dual Mass DCP

Managing Technology Incorporated of Overland Park, Kansas designed and fabricated an ADCP for the Minnesota Department of Transportation. The trailer-mounted device uses hydraulic cylinders to erect the test frame and to automatically lift the hammer. The hammer falls freely, and the number of hammer blows and penetration for each blow are automatically recorded on a laptop computer.

The design and fabrication of the ADCP by Vertek for this project is described later in the Design and Fabrication chapter.

Correlations

Correlations for estimating subgrade soil and paving material strength from cone penetration resistance are most often in the form of equations for CBR as a function of DCP Index (penetration per blow). The following are examples of empirical correlations where DCP Index (DCPI) is expressed in units of millimeters per blow:

$$\text{Log (CBR)} = 2.62 - 1.27 \text{ Log (DCPI)} \quad (1)$$
(Ref. 4)

$$\text{Log (CBR)} = 2.56 - 1.15 \text{ Log (DCPI)} \quad (2)$$
(Ref. 8)

$$\text{CBR} = 269/\text{DCPI} \quad (3)$$
(Ref. 9)

$$\text{Log (CBR)} = 2.20 - 0.71 [\text{Log (DCPI)}]^{1.5} \quad (4)$$
(Ref. 10)

$$\text{Log (CBR)} = 2.81 - 1.32 \text{ Log (DCPI)} \quad (5)$$
(Ref. 11)

$$\text{Log (CBR)} = 2.669 - 1.065 \text{ Log (DCPI)} \quad (6)$$
(Ref. 7)

The above correlations are graphically displayed in Figure 2, which illustrates their similarity.

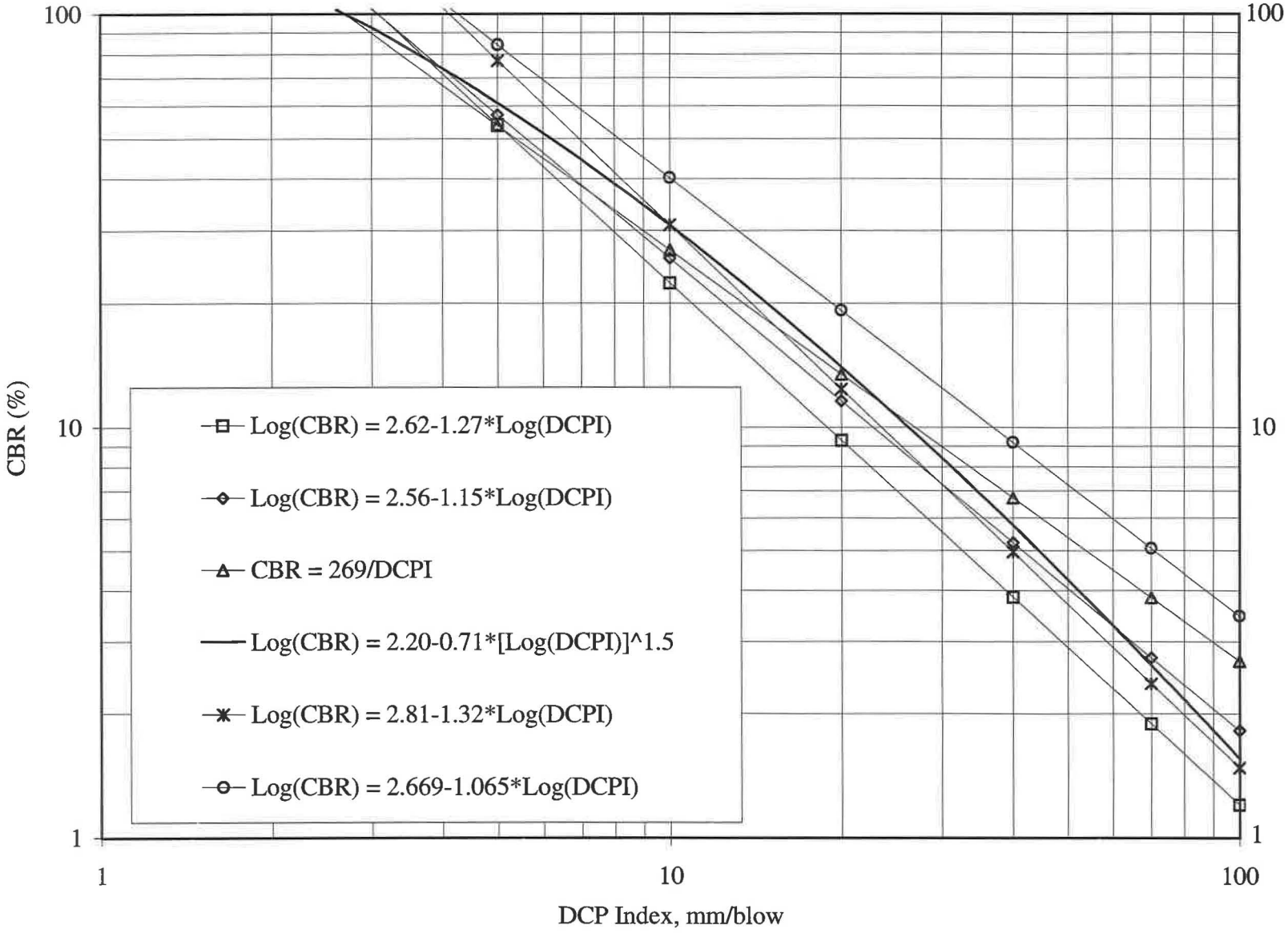

Figure 2. Various Correlations for Estimating CBR from DCPI

The following correlation, proposed by Webster, Grau and Williams (5), was adopted for use in the analysis software for the ADCP developed by Vertek:

$$CBR = 292/(DCPI)^{1.12} \quad (7)$$

The above equation is shown in Figure 3 along with the data used for its development. Comparison with Figure 2 indicates similarity with those correlations. Also shown in Figure 3 are the following relationships for high plasticity clay soils (CH) and low plasticity clay soils (CL) with CBR<10 proposed by Webster, Brown and Porter (12):

$$CBR = 1/(0.002871DCPI) \quad (8)$$

$$CBR = 1/(0.017019DCPI)^2 \quad (9)$$

Any of the above equations may be converted to directly compute limerock bearing ratio (LBR) by substitution of

$$CBR = LBR/1.25 \quad (10)$$

With this substitution the equation used in the analysis software becomes

$$LBR = 365/(DCPI)^{1.12} \quad (11)$$

The equations presented above were developed for the manual DCP, and some corrections may need to be applied when using DCPI measured with the automated DCP. Ese, Myre, Noss and Vaerness (7) report, for the Norwegian ADCP, that the automated and manual DCP yield practically identical results. Livneh, Ishai and Livneh (6) indicate that CBR computed with equation 4 and DCPI from the Israeli ADCP are about 15% larger than CBR computed using DCPI from the manual DCP.

Data and analysis from field and test pit studies will determine if modifications to equations 7 and 11 are needed to account for properties of typical Florida DOT subgrade and paving materials and DCPI measured with the Florida DOT ADCP.

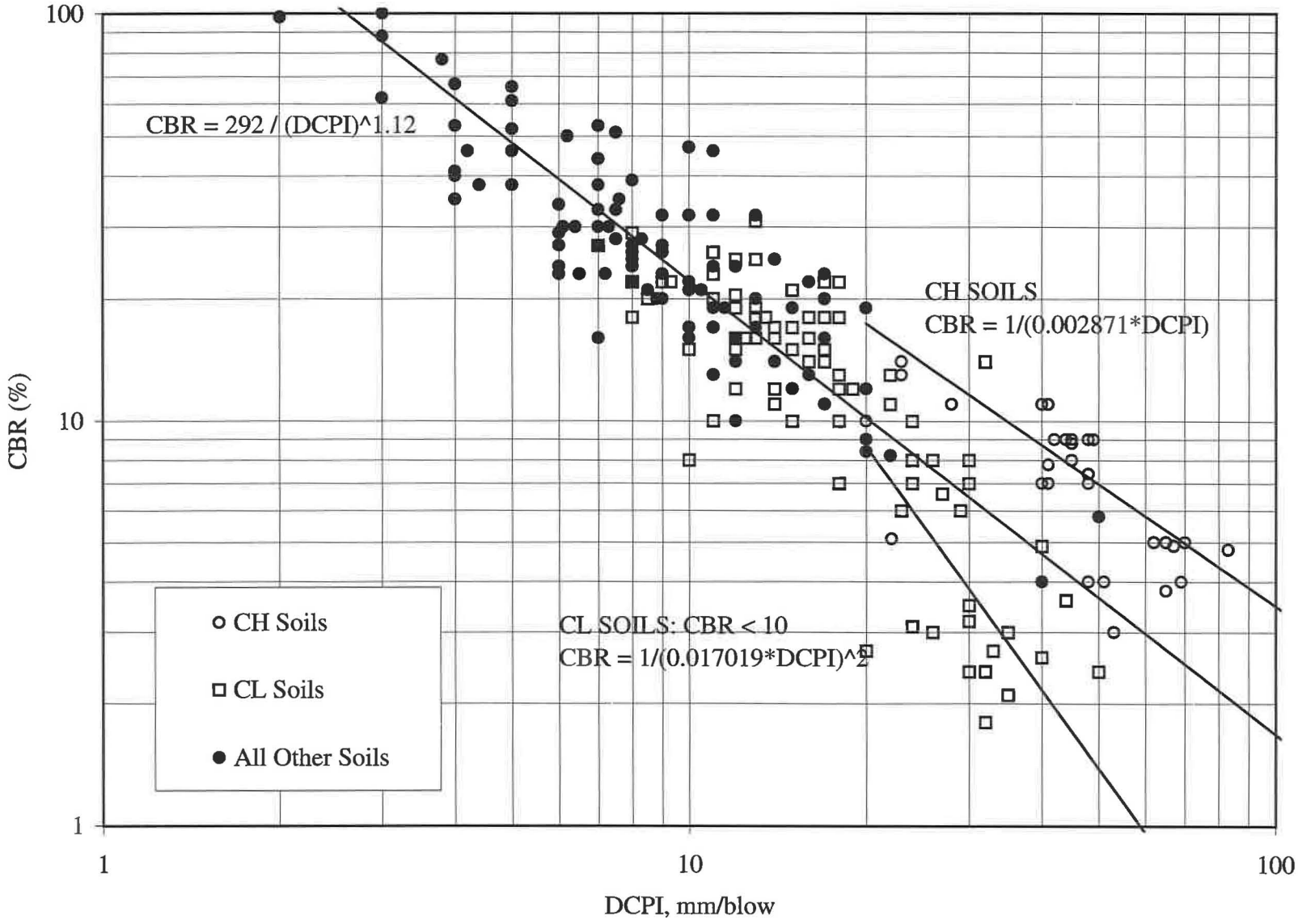

Figure 3. CBR vs DCPI Correlation Adopted from Webster Grau and Williams (5)

Applications

The ADCP can be used to evaluate granular bases, granular subbases and subgrades in existing pavements or in these pavement elements as they are constructed. Applications to evaluate existing pavements are relatively straight forward requiring only coring through asphalt concrete or Portland cement concrete surface layers to provide access to underlying layers. The cone penetrometer can then be driven through base and subbase layers into the subgrade. The in-place pavement structure provides real confinement conditions.

The time for testing can be selected to evaluate the effect of moisture. A worst case condition when water contents are highest may be selected, or tests may be conducted several times during a year to provide data for an average or effective strength assessment as recommended in the 1993 AASHTO pavement design guide (13).

Evaluation of the strength of pavement elements during construction for comparison with design strength assumptions are not as straight forward. Evaluation is normally desired before subsequent layers are placed so that corrective action can be taken if specification requirements are not met. This means that confinement from above layers that is simulated in laboratory tests is not present. For soils and paving materials whose strength is derived primarily from cohesion, lack of confinement may not be a significant factor. But, for granular soils and paving materials whose strength is derived primarily from friction, confinement may have to be provided for realistic strength assessment.

Water contents in as constructed pavement elements will likely be at or near optimum in order to facilitate achieving required compaction levels. However, these water contents will likely be lower than soaked laboratory samples tested for selecting design CBR's. Some form of correction to field CBR's estimated with ADCP, based on water contents, will be needed for comparison with design CBR's to accept or reject as constructed paving materials and subgrades.

OBJECTIVE

The objective of this study was to develop an ADCP and procedures for its use to evaluate in situ strength of Florida DOT granular pavement construction materials and subgrade soils.

SCOPE

To accomplish study objective the following tasks were completed:

1. A review of literature related to DCP use for evaluating paving materials and soils, and automation of the DCP,
2. Design and fabrication of an ADCP with an operation manual,
3. Demonstration and calibration tests with the ADCP in typical Florida paving materials and subgrade soils,
4. Analysis of data from demonstration and calibration tests to formulate recommended correlations between DCPI and LBR, and
5. Preparation of a final report.

ADCP DESIGN AND FABRICATION

Design Criteria

Designed and constructed for one-man operation, quick set-up and simple operation, and automatic data collection, the ADCP produces the same measurements as the standard manual DCP in a more efficient and cost-effective manner. It is designed to perform the tasks of lifting and dropping the weight, recording the number of blows and penetration, and extracting the rod after the testing is complete. The following features were included in the ADCP design:

- 60°, 20 mm, (0.79 in.) diameter conical tip on a 15.9-mm (0.62 in.) rod;
- maximum depth of penetration of 1 m (39 in).;
- rod held in a vertical orientation with level indicator;
- 8.0 kg (17.6 lb) hammer dropped a distance of 575 mm (22.6 in);
- anvil on which the hammer drops advances along with the penetrometer;
- penetration depth is measured and recorded along with blow count;
- automated mechanism for extraction of the penetrometer from the ground;
- operable from 12 V/DC power or 110 V 60-cycle power;
- portable computer with compatible software formated for automated data acquisition, data storage, and data analysis;
- mounted on single-axle trailer capable of being towed into position with a standard ball hitch;
- trailer assembly light enough to be moved manually;
- capability to automatically adjust the energy imparted to the DCP rod by adjusting drop height and or hammer mass;
- capability to shift the mechanism through a 305 mm (12 in.) range parallel to the trailer axle;
- set-up time over the test location should be less than one minute; and
- hammer drop rate between 55 and 70 blows per minute.

Design Considerations

The ADCP operating system performs the following functions:

- raise the drop hammer;
- release the drop hammer;
- measure the depth;
- count hammer blows;
- retract the penetrometer at the conclusion of a test; and
- control sequencing of the various operations.

Based on these requirements, an overall architecture for the test apparatus was developed. A schematic of the ADCP is shown in Figure 4 and Figure 5 is a photograph of the ADCP in operation. The mechanical components of the system are mounted on a mast attached to the trailer. A mechanism to lift and release the drop hammer is mounted to a carriage which moves, under power, up and down along the mast. As a test is being performed, the carriage is controlled in such a way that it always remains in the same position relative to the penetrometer. Thus, the carriage moves down as the penetrometer is advanced into the ground under the action of the hammer blows. After a blow, there is some delay while the carriage catches up with the penetrometer, and the control system must insure that the weight is not dropped again until the carriage is in position. The motion of the carriage thus mimics the motion of the penetrometer. This is important for two reasons. First, the depth of penetration can be determined by measuring the movement of the carriage, thus avoiding the necessity of attaching a measuring device to the penetrometer that will be impacted by the drop hammer. Second, the hammer can be positioned relative to the carriage, which is convenient because the lift mechanism is mounted to the carriage. Since the carriage follows the motion of the penetrometer into the ground, the same mechanism that advances the carriage is designed to retract the penetrometer at the conclusion of the test.

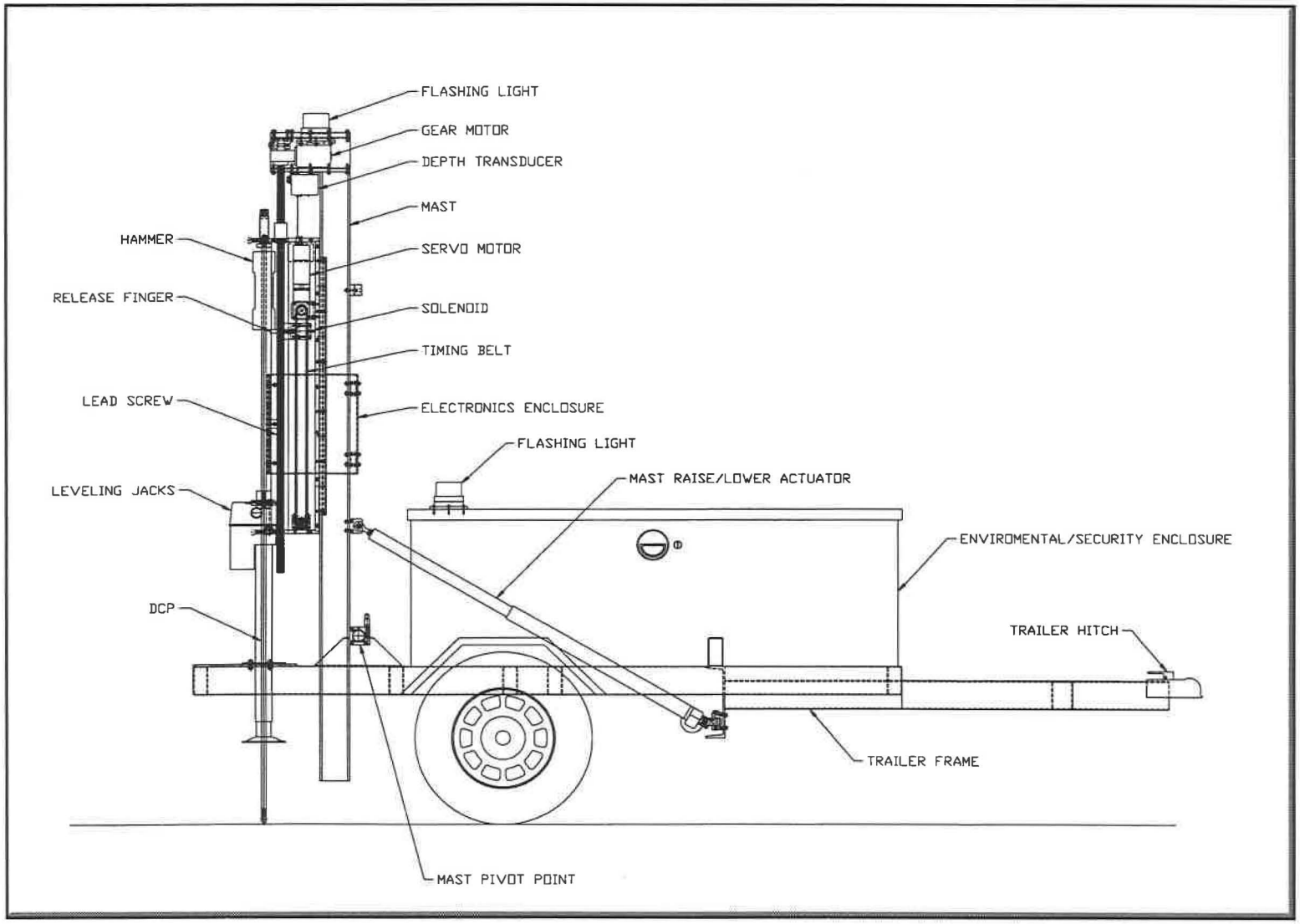

Figure 4. Schematic of ADCP

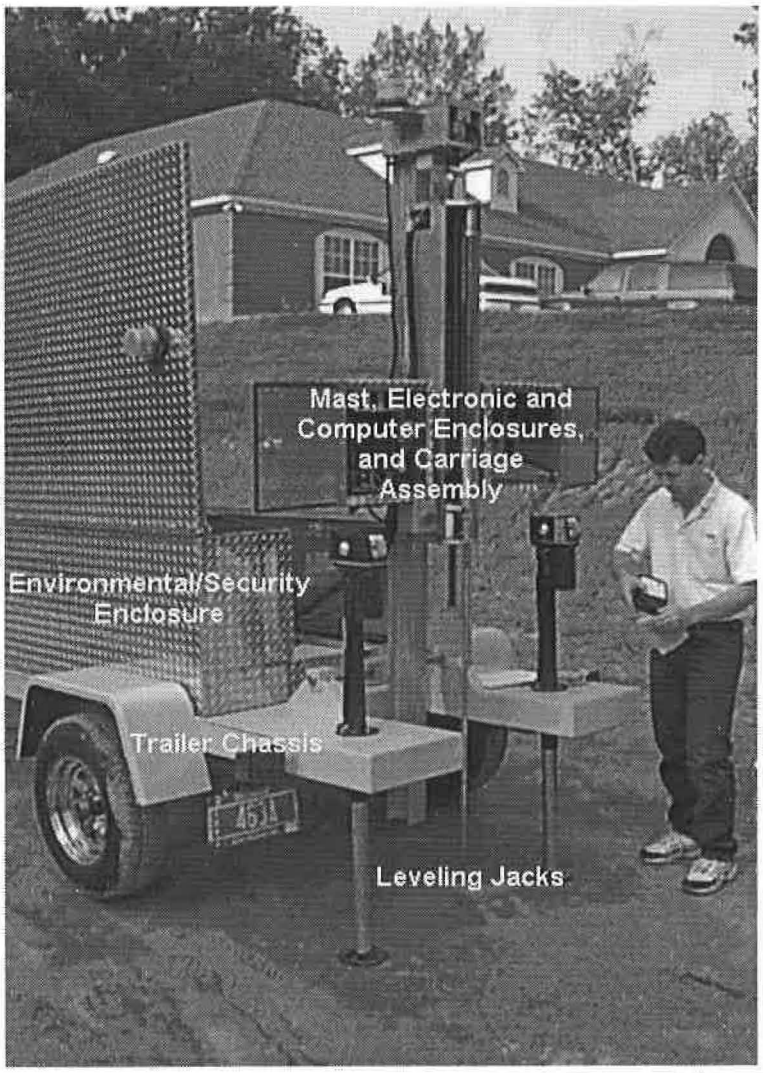

Figure 5. Photograph of ACDP Trailer Prepared for Conducting

Trailer

The ADCP device is permanently mounted on a single axle trailer that can be towed with an automobile or light truck using a standard ball hitch. A durable aluminum box, referred to as the environmental/security enclosure, is rigidly mounted to the trailer chassis. This enclosure has a locking hinged lid that opens from the top, providing a secure enclosure to protect the ACDP device from weather and dust during highway transport and storage. An opening in the rear of the enclosure is fitted with a removable panel. This panel, which should be in place when the ADCP is stowed, is removed when the ADCP is prepared for testing. Two electrically operated jacks on the rear and one manually operated jack on the front of the trailer chassis are provided for elevating, leveling, and stabilizing the trailer during testing. The trailer is furnished with brake and turn signal lighting and is fully road-worthy for transport on public highways. A flashing strobe light is mounted to the enclosure. A locking key switch on the environmental/security enclosure operates the flashing light.

Mast

The mast, which forms the backbone of the ADCP, consists of a single 4-inch deep aluminum wide-flange beam. It is light in weight, but rigid enough to support the DCP apparatus, including the retraction function. One flange of the I-beam also serves as a track on which the carriage is guided. Figure 6 is a photograph of the mast as viewed toward the back of the trailer. The mast retracts into the environmental/security enclosure. The mast is raised and lowered by an electrically operated actuator, identified in Figure 6. This actuator is also used to level the mast prior to conducting a test.

The mast is attached to the trailer by a mast pivot shaft. The mast can be moved on the pivot shaft through a range of motion of 12 in. parallel to the axle of the trailer. Two manual clamps, one on either side of the mast, lock the mast in place on the support bar. When these clamps

are loosened, the mast can be moved manually along the pivot shaft. This feature allows up to three tests to be conducted at a site without moving the trailer.

Two enclosures are attached to the mast assembly: one for housing a portable laptop computer, and one for housing the electronics and control components. The top of the mast is equipped with a second safety strobe light that operates when the mast is erected.

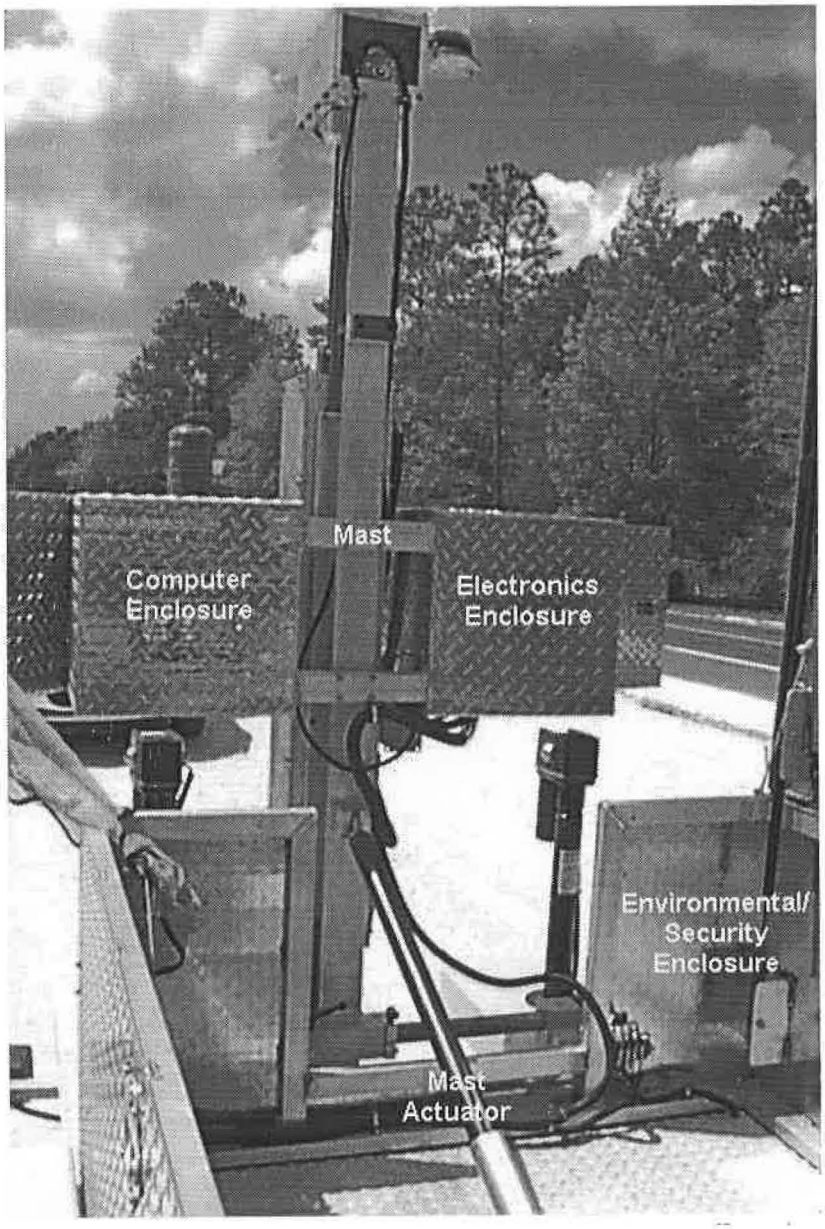

Figure 6. Rear View of ADCP Trailer

Hammer Lift Mechanism

A mechanism to lift and release the drop hammer forms the fundamental component of the system. Because the available energy source is electric power, a hydraulic or pneumatic cylinder-based actuator was not appropriate for this application. The use of a hydraulic or pneumatic cylinder would require inclusion of a hydraulic pump and reservoir or an air compressor for energy conversion, which conflicts with the requirement for light weight and portability. Thus, an electric motor was selected to raise the hammer. The relatively high velocity and low force suggested the use of a belt or chain drive as opposed to a lead screw in this function.

Several types of electro-mechanical systems were considered for controlling the lift height. The hammer must be moved to the drop position and brought to zero velocity before release. In theory, it should be possible to release the hammer below the required drop height while it still has upward velocity, allowing it to come to a stop at the specified drop location. However, with such an approach, the energy delivered to the penetrometer would be subject to the uncertainties in rod friction and orientation, hammer velocity, etc. A decision was made not to pursue this approach. To reduce the possibility of unseating the penetrometer tip, the system was designed to avoid impacting both the handle at the top of the penetrometer rod and the lift apparatus with the hammer. With these considerations in mind, a servo-motor with an electronic controller commanded through the serial port of the personal computer was chosen to raise and lower the hammer lift mechanism. Based on commands from the computer, the servo motor system moves the hammer with the appropriate acceleration and velocity to bring it to a stop at the specified drop position. While this may appear to be unnecessarily "high tech," it accomplishes the required function very effectively and is consistent in technology levels with the portable computer.

The servo motor is coupled through a 5:1 reduction gear box to two timing belt pulleys, on opposite ends of the same shaft. The timing belts, which run on the two pulleys and two matching idler pulleys at the opposite end of the stroke, are fixed to a lift block. The lift block holds the hammer catch/release mechanism and slides along two guide rods. Thus, the motor rotation must be reversed so that each end of the lift stroke reverses the direction of the lift block containing the catch/release mechanism.

Hammer Catch/Release Mechanism

The hammer catch/release mechanism lifts the hammer off of the anvil at the bottom of the lift stroke and releases it at a prescribed distance above the anvil. A solenoid-actuated bracket, called the release finger, which slips under the bottom of the drop hammer, performs this function. Prior to lifting the hammer, the solenoid is actuated to retract the release finger, and the lift block is moved down so that the release finger is below the bottom of the weight. The solenoid is then de-energized, allowing the spring-loaded release finger to extend under the hammer. The lift block is subsequently raised by the servo motor to the specified drop position. To drop the hammer, the solenoid is energized, retracting it from beneath the hammer. It remains retracted until positioned beneath the hammer in preparation for another lift.

Carriage Positioning

The carriage positioning mechanism serves three functions:

- positions the lift mechanism correctly with respect to the penetrometer rod so the hammer is dropped from the correct height;
- mimics the motion of the penetrometer, making it possible to determine the depth of penetration by measuring the movement of the carriage; and
- retracts the penetrometer from the ground at the conclusion of each test. A gear-motor operated lead screw is employed for this function.

The motor and gearbox are attached to the top of the mast, and the lead screw passes through a mating nut affixed to the carriage. During testing, the carriage is moved down to follow the penetrometer. In this mode, power is applied continuously to the motor with a normally closed proximity detector in series. When the carriage reaches the point where the handle of the penetrometer actuates the proximity detector, the circuit opens, stopping the motor with the carriage in the correct position relative to the penetrometer. For retraction, the motor is reversed and run continuously until the depth transducer indicates that it is at the top of its stroke. At this position, the computer turns off the power to the motor. Figure 7 is a close-up photograph of the carriage components.

Depth Measurement

A displacement transducer mounted between the mast and the carriage determines the depth of penetration. A "string potentiometer" type displacement transducer, a simple and effective displacement measurement device, is used for this purpose. It consists of a 10-turn potentiometer attached to a spool with a torsion spring, all of which are enclosed in a metal housing. A thin wire is wound on the spool with its end outside the housing. Pulling on the end of the wire turns the spool, resulting in a change in resistance in the potentiometer. An analog voltage proportional to the wire extension is produced. When the end of the wire is allowed to return, it is retracted under the action of the torsion spring. The potentiometer will break if the wire is caught and pulled out of the housing or is allowed to spring back uncontrolled. In the ADCP, it is situated so that it is well protected by the other rigid metal parts of the system. In normal operation there is no reason to ever disconnect the end of the wire from its attachment point.

A rotary encoder on the lead screw could also serve this function. The disadvantage of this approach is that the encoder can only sense changes in position relative to where it was when

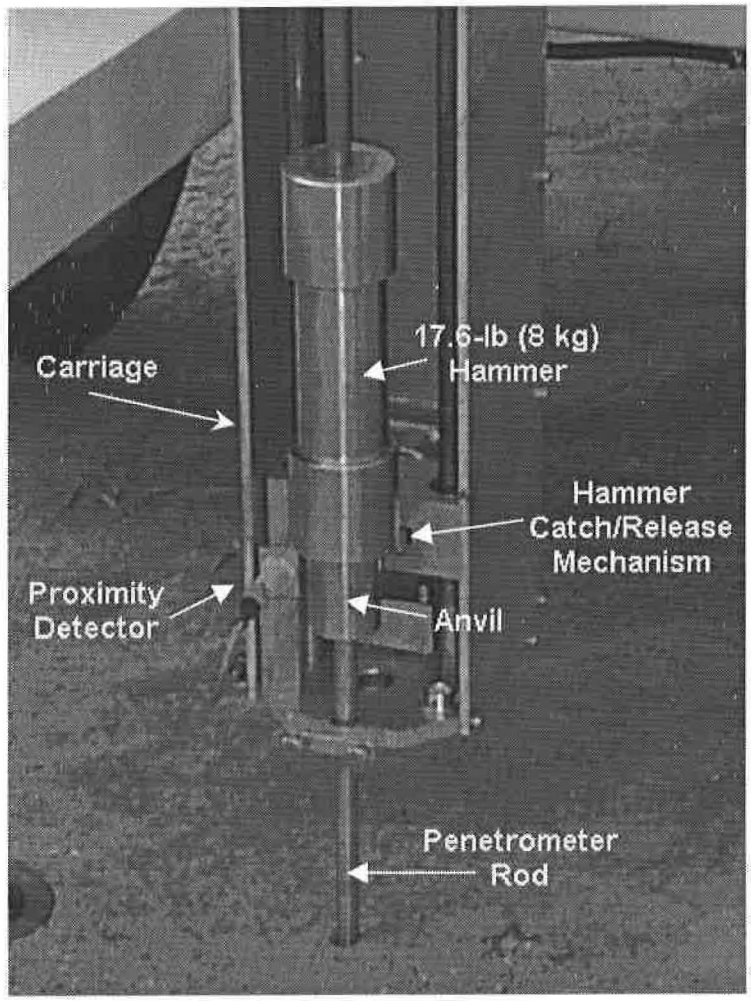

Figure 7. Close-up Photograph of the Carriage Components During Test Conduct

the system was turned on or when the counter was re-zeroed. Thus, if the power is interrupted during a test, it will not be possible to restart the test without returning the carriage to its home position. In contrast, with the string potentiometer, a given output voltage always corresponds to a specific position of the carriage.

Penetrometer

The penetrometer and drop hammer are substantially similar to the standard manually operated version. Because the servo motor controls the lift height of the drop hammer, the distance between the anvil and the top handle is not used to gage the drop height as it is in manual operation. Thus, it was made 10 mm (0.4 in.) longer so there is no possibility of the hammer impacting the handle if there is a slight error in lift height. The bottom section of the rod must be longer than the maximum penetration depth by an amount equal to the maximum allowable penetration on one blow, in this case 75 mm (3 in.). This is necessary because the bottom rod passes through a guide at the bottom of the carriage and the bottom of the anvil must be at least 4 in above the guide prior to each hammer blow.

Because the ADCP includes the capability to mechanically extract the DCP from the ground at the conclusion of a test, there will probably be no reason to use disposable tips, which are currently used with the manual DCP to make to extraction easier.

Control and Data Acquisition System

Control of the various mechanical functions, counting blows, and measurement and recording of penetration depth are accomplished with a laptop computer. The computer's parallel and serial ports are used to perform all interfacing between the other system components. The servo motor controller is commanded through the serial port. All other functions are performed through a combination analog-to-digital converter (ADC) and digital input/output (DIO) card that communicates through the parallel port. One analog channel is used to read the depth

transducer measurement. Three digital outputs are used to actuate relays that control the release finger solenoid, carriage up, and carriage down functions. One digital input is used during testing to let the computer know when the carriage has caught up with the penetrometer after each hammer blow. One additional control component is a proximity detector that provides a "home" signal to the servo motor controller at the beginning of each test.

A single computer program performs all control and data acquisition functions. This program was written in Hewlett Packard VEE, a high level Windows based language that is designed for real time applications.

Power Supplies

All of the electrical/electronic components of the ADCP system, as currently configured, are powered by a single 110 V/AC power source. This approach was followed because the servo-controlled motor was selected for lifting the hammer. One of the features of the servo motor is a very high power density, i.e. high output power for the volume and mass of the motor. This results, in part, from the fact that the motor controller operates with approximately 90 V/DC internal power, which it creates from the standard 110 V/AC input power. It is theoretically possible to control the servo motor with a controller powered by 90 V/DC. However, this is not practical for two reasons. First, the vehicles from which power will be drawn in actual operation do not have these high DC voltages readily available; and second, a commercial off-the-shelf motor controller that uses that input power is not commonly available. Once it was established that 110 V/AC would be used to power the servo motor controller, the decision was made to power the entire system with that voltage. In order to obtain the required 110 V/AC power in the field, the control system was packaged with an electronic inverter that supplies the required power using 12 V/DC as input. For emergency operations, the trailer is fitted with a conventional 12-V automotive battery that can be recharged with 110 V/AC power.

ADCP OPERATION

Preparation

Required Tools

1. Pipe wrench (1/2" opening, 2 required)
2. Adjustable wrench (1-7/8" opening)
3. 1/2" wrench
4. De-burring files
5. Wire brush
6. Light lubricating oil (30W)
7. Automotive-style grease gun with automotive grease

General Precautions

1. All threads on the DCP shaft should be clean and free of contaminants. Dirty threads can fail to seat properly, resulting in possible failure of the DCP probe.

2. Before testing, check that all threaded connections are tight, including the tip. Be careful not to raise burrs on the tip when tightening.

3. Take care to avoid injury from sharp burrs when handling and loading the DCP probe.

4. Stay clear of all pinch points and use extra precaution to keep hands and loose articles away from all moving parts.

DCP Probe Assembly

1. Refer to Figure 8.

2. After cleaning threads, install the tip (1) into lower anvil assembly (2). Tighten together with two pipe wrenches being cautious not to burr the tip (1) or the lower anvil assembly (2).

3. Slide the desired hammer onto the upper handle assembly (4). Two hammers are provided, one weighing 8 kg (17.6 lbs) (3) and the other weighing 4.6 kg (10.1 lbs) (3).

4. Screw together the lower anvil assembly (2) with tip (1) installed and the upper handle assembly (4) with desired weight (3) using precautions not to allow weight to slide down the upper handle assembly (4) which could cause injury (one way to avoid this is to assemble probe upside down)

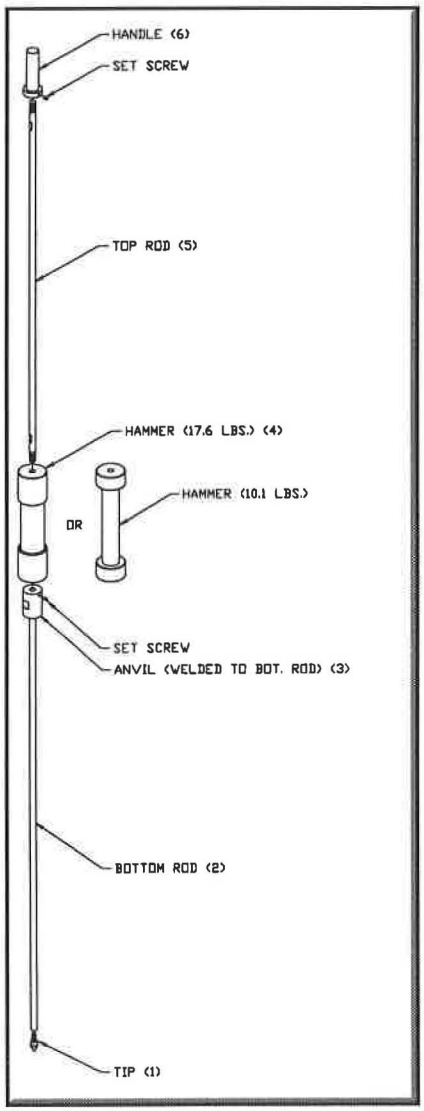

Figure 8. DCP Probe Assembly Diagram

Operating Procedure

1. Obtain utility clearance prior to conducting any test.

2. Locate trailer near or at test location.

3. Tilt front trailer jack 90° and lower to ground to stabilize front of trailer.

4. Unlock and open environmental/security enclosure lid to full extension.

5. Remove rear panel of environmental/security enclosure and store in a secure location.

6. Release EMERGENCY STOP button located on the carriage assembly and place INVERTER SWITCH in the "ON" position and MAIN POWER SWITCH in the "ON" position.

7. Lower both rear trailer jacks until both trailer wheels are off the ground.

8. Loosen two clamping handles on the mast main pivot shaft.

9. Using the MAST RAISE AND LOWER ROCKER SWITCH, located on the side of the right rear jack, raise the DCP mast to vertical position.

10. Close main enclosure lid.

11. Use BULLSEYE LEVEL located on the lower right corner of the carriage assembly to plumb the DCP mast by adjusting the height of the two rear jacks and angle of the DCP mast.

12. Open the right hand enclosure and install portable personal computer. Make sure all electrical connections are plugged in properly and secured.

13. Open the left hand or electronics enclosure. Move the AC POWER switch and the DC POWER switch to their "ON" positions.

14. Raise carriage assembly to the highest load position by switching CARRIAGE AUTO/MANUAL rocker switch to "MANUAL" and press "UP" on the CARRIAGE UP/DOWN rocker switch. When carriage stops moving upward, release rocker switch.

15. Switch CARRIAGE AUTO/MANUAL switch to "AUTO" and close enclosure door. Door should remain closed for entire test to prevent dust and debris from damaging electronics.

16. Remove lower clamping assembly on the carriage assembly by removing the two thumb screws.

17. Load the DCP probe assembly into the carriage assembly by sliding the handle portion of the probe up through the upper clamping assembly and resting anvil of the probe on the lower plate of the carriage assembly.

18. Install lower clamping assembly to hold probe in proper location and secure all thumb screws.

19. Locate probe assembly by sliding mast back and forth to proper location and secure position by tightening the two clamping handles.

20. Boot computer in the right hand enclosure. Double click on the ADCP icon on the main screen and follow instructions as provided by the computer. The main screen gives the operator the option of starting a test, exiting the software, or retracting the rod. The operator is also prompted to select the measurement system to use, English or metric. The software will display the selected units but will save the data to file in metric only. The software returns to this screen between tests. Selecting EXIT or pressing F1 will put the DCP in shutdown configuration and exit the software. F1 may be used anytime during the test (but is not recommended.). Pressing F9 will pause the operation of the DCP. The operator then has the option of continuing or ending the test. F9 may be used anytime during the test and is the recommended method of stopping.

21. Select START to begin a test. The User Input Screen is displayed. The following information is written to the header of the data file.

Filename	The name of the data file for this test. A new filename must be entered for each test. Any duplicate filename will overwrite an existing file.
Test ID	Any information concerning the test which needs to be placed in the data file.
Operator	
Test Information	
Soil Type	
Weight Type	DCP mass being used.
Drop Height	The height in mm which the weight is to be dropped.
Max Depth	The maximum depth in mm for the test. This is an end condition and the test will be stopped when this depth is reached. Additional blows can be added after the test has stopped if further penetration is desired.
Max Blows	The maximum number of blows. This is an end condition and the test will be stopped when the specified number of blows has been reached.

22. Select START TEST to begin the test. The DCP will initialize itself by lowering the DCP rod to the ground and positioning the carriage. The motor will seek home position below the weight. The computer screen will display "LOWERING TO GROUND" or "HOMING". Once the system in initialized, the test will automatically begin.

23. The weight will be lifted and dropped and the Blow Count, Depth in mm, and time will be written to the data file every cycle. The current depth in mm (or inches) and blow count is displayed in the screen as the test is running. The test will continue until paused by the operator, the maximum depth is reached, or the maximum blow count is reached. If the system is paused using F9, the operator has the option of continuing the test or ending the test by selecting the appropriate button on the screen.

23. If the maximum depth is reached the test is stopped and the operator will be prompted to end or continue the test. To continue, the operator must specify a new maximum depth. If the maximum blow count is reached the test is stopped and operator will be prompted to end or continue the test. To continue, the operator must specify a new maximum blow count.

24. Once the test is ended, the operator is prompted to retract the rod, the data file is closed, and the software returns to the main screen.

Transporting Procedure

1. Remove portable computer from the right hand enclosure, close and secure door.

2. Switch both A/C AND D/C POWER switches located in the left hand enclosure to the "OFF" position. Close and secure enclosure door.

3. Remove the DCP probe assembly from the carriage assembly. Disassemble probe assembly and return to transport location provided on the inside of the enclosure. The lower anvil assembly must be placed in first with the anvil end being against the rear of the enclosure. Then place upper handle assembly in location with handle end against the front of the enclosure. Secure in place with clamps and thumb screws provided. Slide weight onto transport rod and secure in place with cotter pin provided.

4. Loosen the mast clamping handles and locate mast between two red lines engraved in the mast main pivot shaft. This is very important so that there is no obstruction to cause injury or damage when mast is lowered.

5. Open main enclosure lid to full extension.

6. Raise rear trailer jacks as far as they will go to prevent damage during transport.

7. Lower mast by pushing downward on the mast raise/lower rocker switch located on the side of the right rear trailer jack. Lower mast until mast rests on rubber pad provided.

8. Switch the INVERTER and MAIN POWER switch to the "OFF" position.

9. Push in the EMERGENCY STOP button located on the main carriage assembly. This ensures that all power has been shut down.

10. Replace enclosure rear panel.

11. Close and secure main enclosure lid to prepare the trailer for transport.

Battery Charging Procedure

1. Open main enclosure lid to full extension and release the EMERGENCY STOP button by turning the button and causing it to pop out. This turns on the emergency stop solenoid which enables the inverter/charger to charge the battery.

2. Close and secure main enclosure lid.

3. Plug in 110 VAC power chord to the receptacle provided on the front right corner of main enclosure. This will charge the on board battery.

Routine Maintenance Procedures

Trailer Maintenance

1. Check ball coupler for operation.

2. Check safety chains for damage or wear.

3. Grease main axle bearings (grease fittings provided on both ends of axle).

4. Keep battery fully charged.

5. Keep lights running properly.

Main Mast Maintenance

1. Apply light coat of 30W oil to main pivot shaft.

2. Apply light coat of 30W oil to carriage slide shafts.

3. Apply light coat of 30W oil to guide surface for main carriage on main wide-flange beam.

4. Grease main screw mechanism for lowering and raising the carriage assembly.

5. Check belts for damage or wear.

6. Weight release finger should slide freely.

TEST PIT AND FIELD STUDIES

A series of test pit and field studies were conducted to demonstrate features and capabilities of the ADCP and to calibrate predictive correlations for typical Florida paving materials and subgrade soils. Field studies were conducted on pavement construction projects and test pit studies were conducted at the Florida DOT State Materials Office in Gainesville.

Test Pit Descriptions

The Florida DOT test pit facility is designed for constructing and testing soils and paving materials under controlled conditions. The concrete pit is located in a building and has dimensions shown in Figure 9. The soils and/or paving materials were spread and compacted in 5 - 6 in. lifts on an A-3 sand subgrade. Three sections (East, Center and West), comprised of different soils or paving materials, were constructed and tested in two series as outlined in Table 1. Water content, density and LBR tests were conducted as each lift of soil or paving material

Table 1. Test Pit Studies

Series	Section	Description
1	East	A-2-4 Sand with Rock
1	Center	A-2-4 Clayey Sand
1	West	A-2-4 Clayey Sand
2	East	A-2-4 Marl
2	Center	12 in. Limerock Base on 12 in. Limerock Stabilized A-3 Sand
2	West	A-1-b Coarse Sand
2	West Modified	5 in. Limerock Base on A-1-b Coarse Sand

was placed. Averages from these tests are shown in Table 2. Similar data from laboratory tests and tests conducted in trenches excavated after completion of DCP testing (designated as "At Testing") are also tabulated in Table 2.

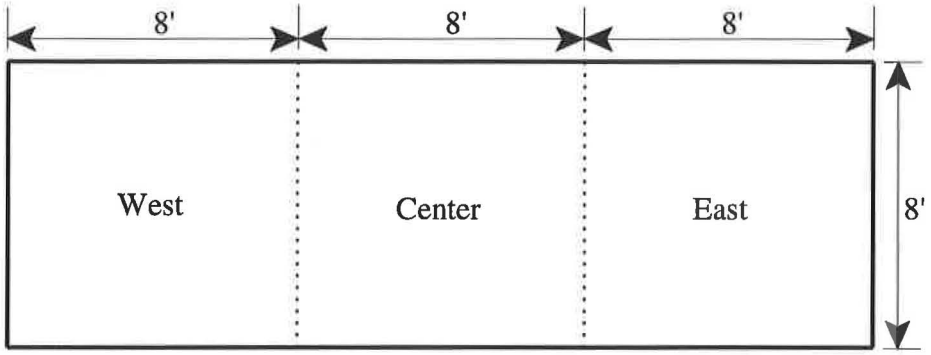

Plan

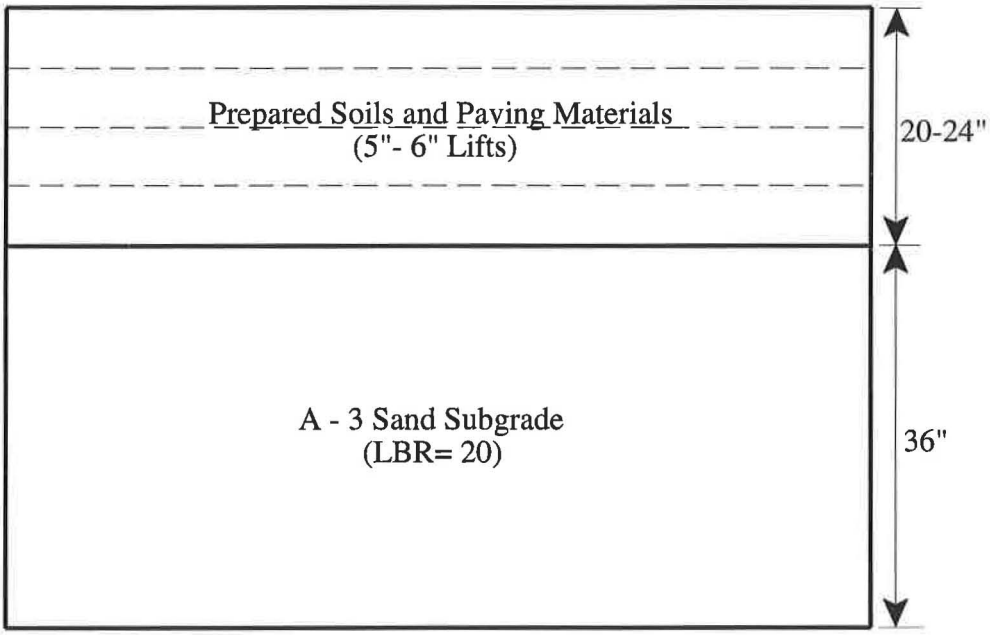

Elevation

Figure 9. Test Pit Layout

Table 2. Laboratory and Field LBR Data

Description	Soil Classification	Laboratory			As Constructed			At Testing		
		w, %	γ_d, pcf	LBR	w, %	γ_d, pcf	LBR	w, %	γ_d, pcf	LBR
Test Pit, Series 1, East Section	A-2-4 (13)*	9.2	119.2	45	7.3	96.3	10	5.8	--	39
Test Pit, Series 1, Center Section	A-2-4 (13)	7.1	119.5	75	7.4	97.4	32	5.1	--	104
Test Pit, Series 1, West Section	A-2-4 (29)	10.3	121.7	75	9.8	96.6	27	6.9	--	79
I-75, LR Base Section	L R Base	--	--	--	--	--	--	--	--	55
I-75, LR Base Section	Stab. s.g.	—	--	83	--	--	--	--	--	--
I-75, Stab. s.g. Section	Stab. s.g.	—	--	83	--	--	--	--	--	--
I-75, Sand s.g. Section	A-3	--	--	--	--	--	--	--	--	35
Test Pit, Series 2, East Section	A-2-4 (24)	8.5	128.7	126		124.1	40	--	--	71
Test Pit, Series 2, Center Section	LR Base	10.3	122.2	129		121.8	30	--	--	32
Test Pit, Series 2, Center Section	LR Stab. s.g., A-3 (8)	9.5	113.5	52		113.4	24	--	--	52
Test Pit, Series 2, West Section	A-1-b (1)	11.3	105.7	26		104.7	7	--	--	--
SR326, LR Base & Stab. s.g.	LR Stab. s.g.	--	—	70	--	--	--	--	--	--
SR26, LR Base & Stab. s.g.	LR Stab. s.g.	12	121	72	--	--	--	--	--	--

*Values in parentheses following classifications are % passing #200 sieve.

Field Test Descriptions

Testing was conducted on pavement construction projects on I-75 in Hamilton County, on SR326 near Ocala, and on SR26 near Gainesville. Pertinent project features are tabulated in Table 3. The three sections on the I-75 projects were completed to specifications through the limerock base, stabilized subgrade and unstabilized subgrade as described in Table 3. The distinguishing feature of the SR 326 project section was that the top 6 in. lift of a 12 in. limerock base was in place, but specified density had not been achieved. Two sections on the SR 26 project had 10 and 7 in. limerock base layers. Specified density had been achieved in the 10 in. limerock base layer, but not in the 7 in. limerock base layer. Limited laboratory moisture, density and LBR data for the stabilized subgrade layers on the field projects are included in Table 2. Field LBR values, run at the time of ADCP testing, are shown for the I-75 limerock base and sand subgrade sections. No field LBR tests were run on the I-75 stabilized subgrade section, the SR 326 project or the SR26 project.

Table 3. Field Studies

Location	Section	Description
I-75	LR Base	12.5 in. LR Base over 12" Stab. s.g.
I-75	Stab. s.g.	12 in. Stab. s.g.
I-75	Sand s.g.	A-3 Sand Subgrade
SR326	LR Base	12 in. LR Base over 12 in. LR Stab. s.g. Top 6 in. lift of LR Base not @ specified density.
SR326	10 in. LR Base	10 in. LR Base over 12 in. LR Stab. s.g.
SR326	7 in. LR Base	7 in. LR Base over 12 in. LR Stab. s.g. LR Base not @ specified density.

DCP Testing

Manual and automated DCP tests were conducted in the test pits. The DCP was driven full depth through the 20-24 in. of prepared soil or paving material into the sand subgrade. Average

LBR values predicted with Equation 11 are summarized in Table 4. Averages for the entire and middle half depth are shown, except for the series 2, West Section, A-1-b sand. Consistent increases in LBR with depth that reflect the influence of confinement were observed for sands. For the A-1-b sand, averages for the top 6" and 12" are shown for comparisons.

Only the ADCP was run during the field tests. At sections containing base and/or stabilized subgrade, the DCP was driven through the paving layers into the subgrade. At the I-75, A-3 sand section, the DCP was driven approximately 24 in. (600 mm).

Average LBR values predicted with Equation 11 are shown in Table 4 for the field sections. As with the test pit studies, averages for full and middle half depths are shown. An exception is the I-75, A-3 sand subgrade section where averages for the top 6 and 12 in. are shown.

To determine if the effects of confinement from overlaying material could be simulated, a series of ADCP tests were run through 3/4 in. dia. holes in 1 and 2 ft. dia. steel plates placed on the surface. The 1 ft. dia. plates were first used on the I-75 field studies and no apparent effect observed. The 2 ft. dia. plates were added for the Series 2 Test pit studies. The plates were stacked to provide surcharge pressures of 0.21 to 0.84 psi. LBR data illustrating the influence of the plates are summarized in Table 5.

After completion of DCP testing on the Series 2 West Section, A-1-b sand, a 5 in. limerock base was constructed to determine if its effects would be different from approximately 0.35 psi pressure from plates. The average LBR from these tests is also shown in Table 5.

Table 4. LBR Predicted from DCPI

Description	LBR from Automated DCP		LBR from Manual DCP	
	Full Depth	Middle Half	Full Depth	Middle Half
Test Pit, Series 1, East Section	28	26	32	29
Test Pit, Series 1, Center Section	46	47	50	52
Test Pit, Series 1, West Section	72	82	71	82
I-75, LR Base Section, LR Base	48	64	--	--
I-75, LR Base Section, Stab. s.g.	48	48	--	--
I-75, Stab. s.g., Section, Stab. s.g.	8	9	--	--
I-75, Sand s.g., Section, A-3 Sand	9*	12**	--	--
Test Pit, Series 2, East Section, Marl	53	59	49	60
Test Pit, Series 2, Ctr. Sec., LR Base	92	90	84	87
Test Pit, Series 2, Ctr. Sec., Stab. s.g.	70	73	80	83
Test Pit, Series 2, West Sec., A-1-b Sand	7*	13**	3*	7**
SR 3226, Top 6" LR Base, No Density	80	82	--	--
SR 3226, Bot. 6" LR Base, Density	134	140	--	--
SR 3226, LR Stab. s.g.	51	50	--	--
SR 26, 10" LR Base, No Density	103	97	--	--
SR 26, LR Stab. s.g.	120	127	--	--
SR 26, 7" LR Base, No Density	65	66	--	--
SR 26, Stab. s.g.	31	26	--	--

*Top 6" (150mm)
**Top 12" (300mm)
Sands show consistent increase in LBR with depth reflecting effects of increased confining stress.

Table 5. LBR Data Demonstrating Effect of Surcharge Pressure

Description	LBR						
	With No. Plates	1' Dia. Plate			2' Dia. Plate		5" LR Base
		0.21 psi	0.42 psi	0.84 psi	0.28 psi	0.49 psi	
I-75, LR Base Sec., LR Base	51	44	--	54	--	--	--
I-75, Stab. s.g. Sec., Stab. s.g.	8	10	10	9	--	--	--
I-75, Sand s.g. Sec., A-3 Sand	8	8	10	9	--	--	--
Test Pit Series 2, East Sec., Marl	63	--	--	--	62	--	--
Test Pit Series 2, Center Sec., LR Base	92	--	--	--	80	--	--
Test Pit Series 2, West Sec., A-1-b Sand	14	--	10	--	10	15	25

LBR values are for 12" LR Base and sta. s.g. layer thicknesses and for the top 12" of subgrades.

ANALYSIS

Data from test pit and field studies were analyzed to demonstrate features and capabilities of the ADCP and to calibrate correlations for predicting strength of typical Florida paving materials and subgrade soils. The following sections will

1. Examine some of the features of pavement strength with depth profiles that may be detected with the ADCP,
2. Compare data from test pit and field studies with correlations for predicting soil and paving material properties from DCPI,
3. Investigate reduced hammer drop heights for soft and weak soils, and
4. Examine the effects of confinement, moisture content and density on strength parameters estimated with DCPI.

Pavement Strength Profiles

Changes in resistance as a cone penetrometer is driven through a pavement structure can provide a strength profile with depth. Typically strength increases as pavement layers are sequentially added above the subgrade. This increasing strength is partially due to increased material quality, but the improved compaction that can be achieved as succeeding layers are placed is also a factor. For granular or cohesionless materials, confinement and, therefore, depth also affects strength. For cohesive materials, confinement has minimal effect on strength.

Figures 10 and 11 are plots of ADCP derived LBR versus depth for Test Pit Series 1, West Section, a clayey sand with 29% passing the #200 sieve and Series 2, East Section, a marl with 24% passing the #200 sieve. These plots illustrate typical profiles for cohesive soils that have relatively uniform strength with depth.

The strength profiles, particularly Figure 10, also illustrate low strength at the top and bottom which is typical for soil and paving materials placed and compacted in layers. The first lift may not achieve complete compaction because of shifting and yielding of the subgrade. Subsequent layers are better compacted as their foundations become stiffer. The top lift may be weaker

because it has received compaction energy only during its compaction, whereas, lower layers receive additional energy from the compaction of above layers. In addition, the top layer has no confinement which may reduce strength.

Figures 12 and 13 illustrate typical strength profiles for cohesionless soils. The indicated increase in strength with depth reflects the obvious increase in confinement with depth. Figure 13 also illustrates the ability of the ADCP to detect abrupt changes in strength that may occur at cut/fill boundaries.

Figures 14 and 15 illustrate strength profiles through limerock base and stabilized subgrade layers. Specified density had been achieved in all layers in Figure 14, and the profile illustrates the increase in strength achieved as layers are added.

The weaker portions, top and bottom, of the 12 ½ in. limerock base are thought to accurately reflect lack of confinement and or compaction, but are typical of good and acceptable limerock base construction. Subsequent placement and compaction of asphalt concrete binder and surface layers would strengthen the top portion of the limerock base layer and it would provide the structural capacity expected of a 12 ½ in., LBR = 100 base course.

The predicted LBR profile through the limerock base layer raises an issue that must be addressed in order to use the ADCP for acceptance during construction. Criteria as to what is acceptable must be set. This will require additional study, but examination of profiles from three field projects suggest the top and bottom 10 to 20% of a layer should not be considered, ie, layer acceptance should be based on achievement of minimum acceptable strength (for example LBR = 100) in the middle 60 to 80% of a layer.

The LBR variation through the limerock base layer in Figure 15 provides a clear illustration of the ability of the ADCP for detecting noncompliant construction. Required density had been achieved in the lower 6 in. lift and this is reflected by LBR $\geq$ 100. Required density had not been

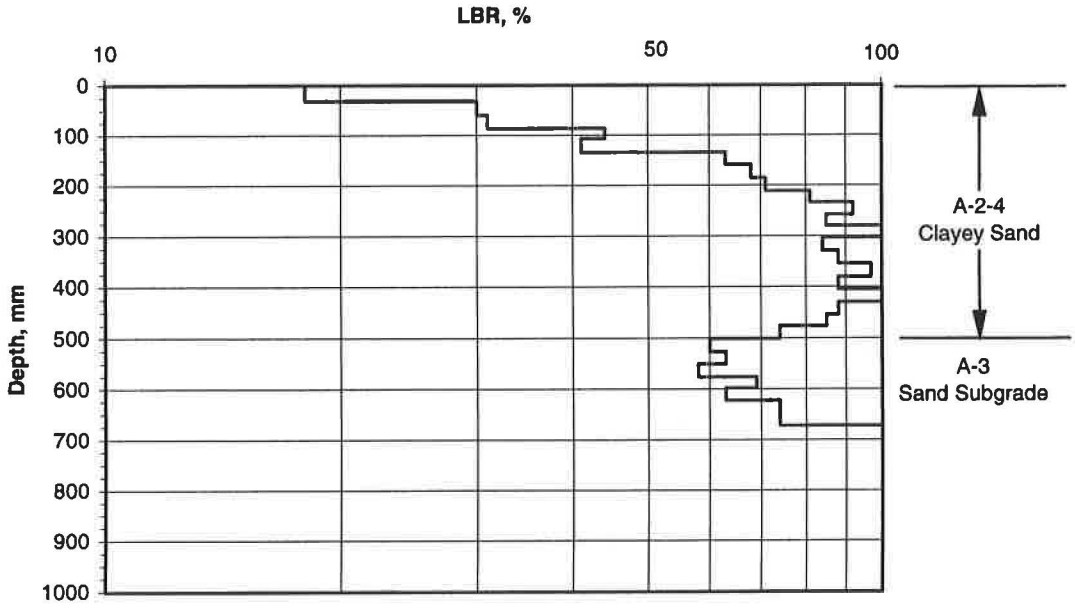

Figure 10. Strength Profile for Test Pit Series 1, West Section, A-2-4 Clayey Sand

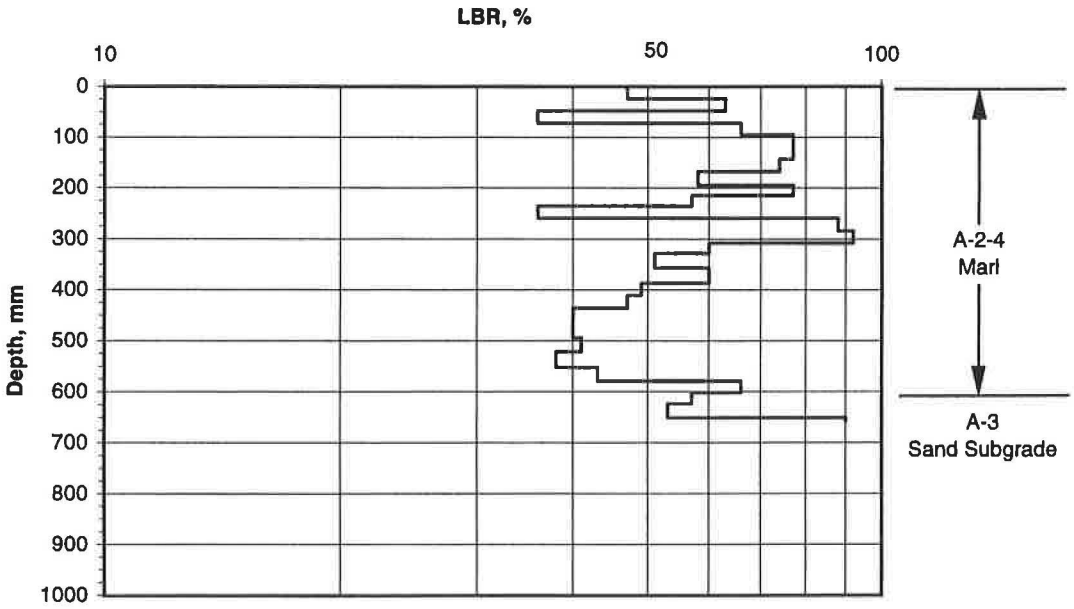

Figure 11. Strength Profile for Test Pit Series 2, East Section, A-2-4 Marl

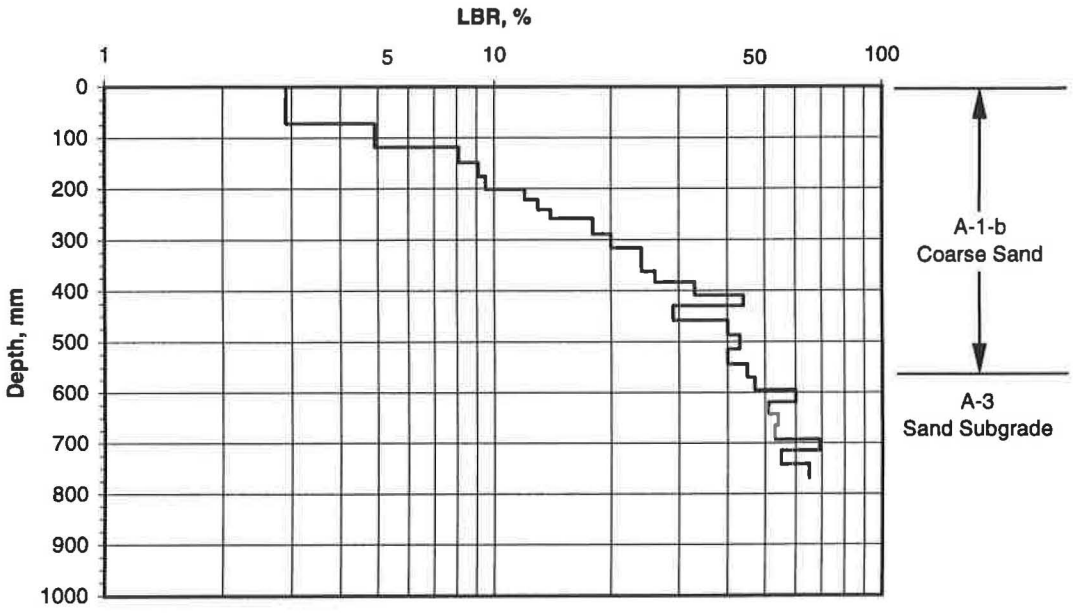

Figure 12. Strength Profile Test Pit Series 2, West Section A-1-b Coarse Sand

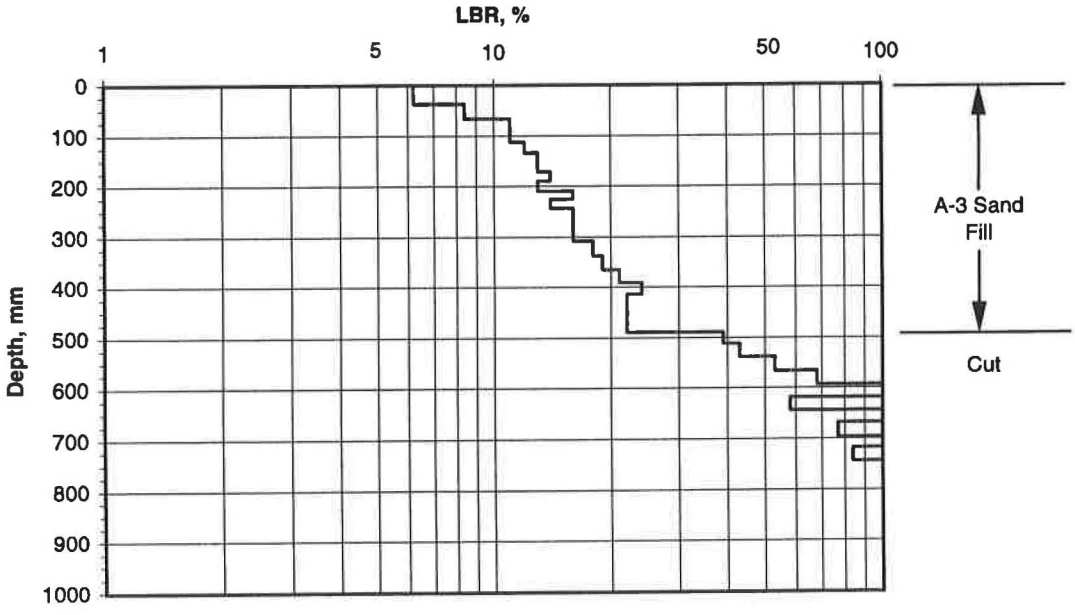

Figure 13. Strength Profile for I-75, A-3 Sand Subgrade Section

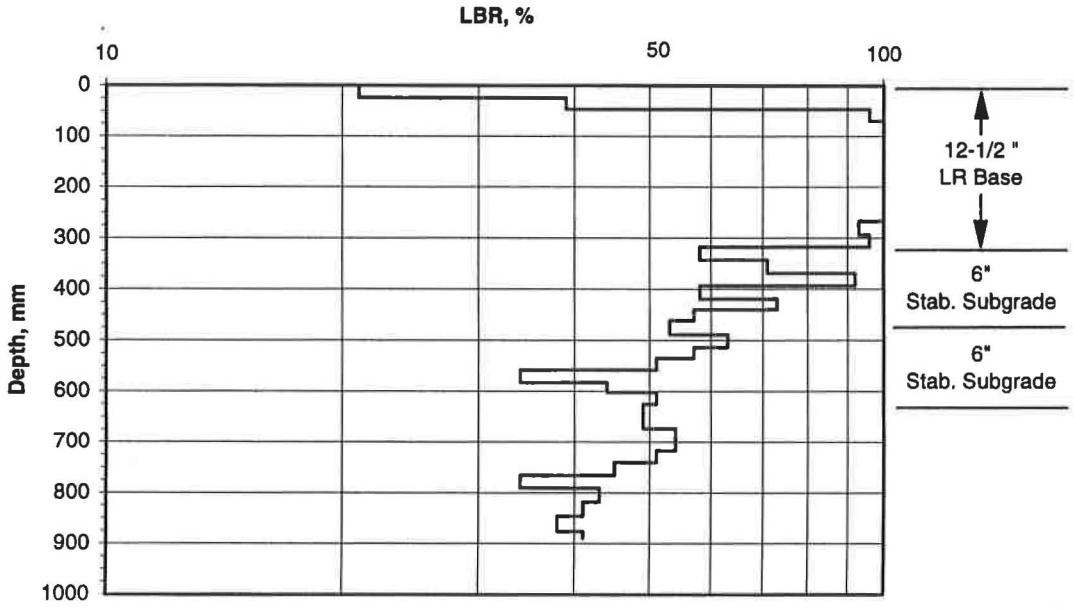

Figure 14. Strength Profile for I-75 LT Base Section

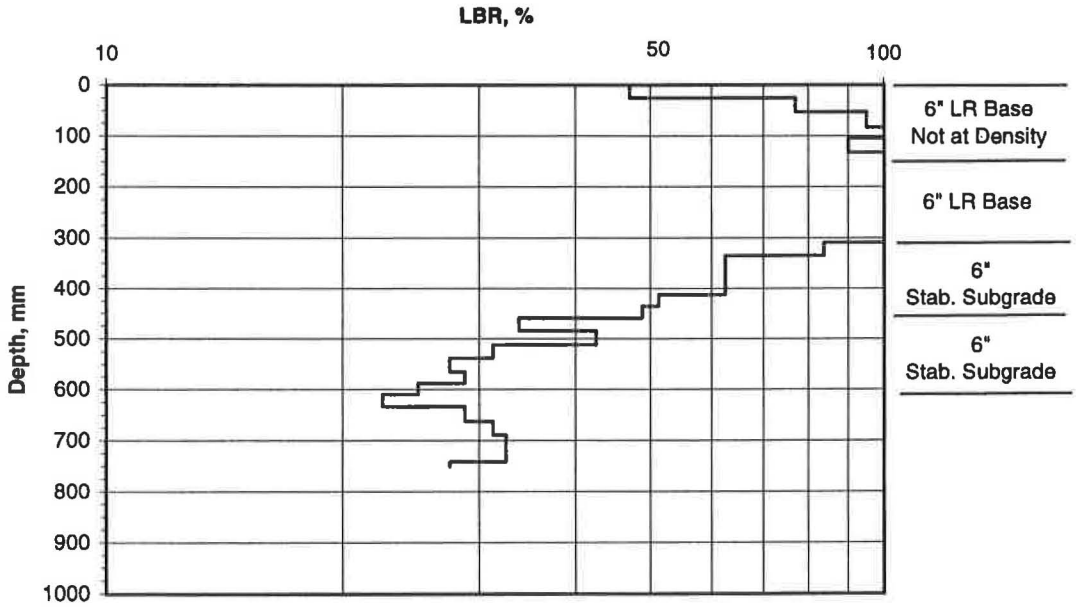

Figure 15. Strength Profile for SR 326, Limerock Base and Limerock Stabilized Subgrade

achieved in the upper 6 in. lift and this is reflected by lower LBR values.

Similar issues of acceptance criteria must be addressed for stabilized subgrade layers. The strength of the stabilized subgrade in Figure 14 decreases with depth which is commensurate with decreased compaction efficiency. Average LBR for the top 6 in. stabilized subgrade layer is about 70 and 55 for the bottom 6 in. layer. These are greater than the required LBR = 40, but there is one increment near the bottom of the lower 6 in. layer that has LBR < 40.

Figure 15 provides a second example. The rate of decrease in strength with depth is greater. The average LBR for the top 6 in. lift of the stabilized subgrade is about 50 and 25 for the bottom 6 in. lift. In addition, most LBR values for the bottom 6 in. lift are less than 40.

The question that must be addressed in order to set criteria for construction acceptance is: what minimum requirements will assure structural capacity expected of a 12 in., LBR = 40, layer? Based on thickness selection methodology, an LBR = 40 measured at the top of the layer may be structurally sufficient. However, additional research is needed to establish requirements for structural adequacy. Possible criteria that is successively more rigorous might include:

1. Average LBR > 40 for the top 6 in. lift,
2. Minimum LBR> 40 for the top 6 in. lift,
3. Average LBR > 40 for the total 12 in. layer, or
4. Minimum LBR > 40 for the total 12 in. layer.

An additional factor that must be considered in setting acceptance criteria is the relationship between laboratory LBR, which is the basis for structural layer thickness design, and field LBR estimated with the ADCP. This issue will be addressed in a subsequent section.

Correlations of DCPI and LBR

The correlation, Equation 7 on page 6, suggested by Webster, Brown and Porter (12), is recommended for estimating CBR from measured DCPI. Equation 10 can be used to convert Equation 7 to Equation 11 for predicting LBR. As noted earlier, Equation 7 was developed with

manual DCPI but data from this study indicates DCPI obtained with the Florida DOT ADCP may also be used to estimate CBR/LBR.

Manual and automated DCP tests were conducted in six of the test pit sections; manual tests were not performed in the Series 2, West Modified Section. Data from these tests were analyzed and show no appreciable difference between manual and automated DCPI. It is, therefore, concluded that automated DCPI can be used in Equation 11 to estimate LBR.

Average plots of blows versus penetration were made for the six test pit sections. Figure 16 and 17 are typical examples that illustrate little difference between cone penetration resistance measured with the manual and automated DCP. The terms n_m and n_a indicate the number of manual and automated tests, respectively, averaged to produce the curves. Data for all six test pit sections are summarized in Figures 18 and 19. Manual and automated DCPI for the 5 to 6 in. lifts used to construct the soils or paving materials in the test pits are plotted in Figure 18 about a line of equality. The data is further condensed in Figure 19 where average LBR's for the entire depth of each soil or paving material is plotted about a line of equality. The LBR's were computed with Equation 11 and are included in Table 4.

The relevance of Equation 11 to Florida soils and paving materials is illustrated in Figure 20. Note that CBR rather than LBR is plotted with DCPI. The CBR's plotted in Figure 20 were measured at about the same time ADCP testing was conducted. Corresponding LBR's are tabulated in Table 2. Values are averages from several tests. For the test pits, trenches were excavated after the ADCP testing and CBR/LBR tests conducted at several depths. For example, the LBR = 39 (CBR = 31) for Test Pit, Series 1, East Section is the average of 11 tests conducted on 4 - 5 in. lifts of soil comprising the section. The corresponding DCPI = 9.9 mm/blow was obtained by averaging six ADCP tests over the full 20 in. depth of the section. Overall, Figure 20 indicates reasonable agreement between Equation 7 and data for Florida soils and paving materials. Therefore, no modifications are recommended.

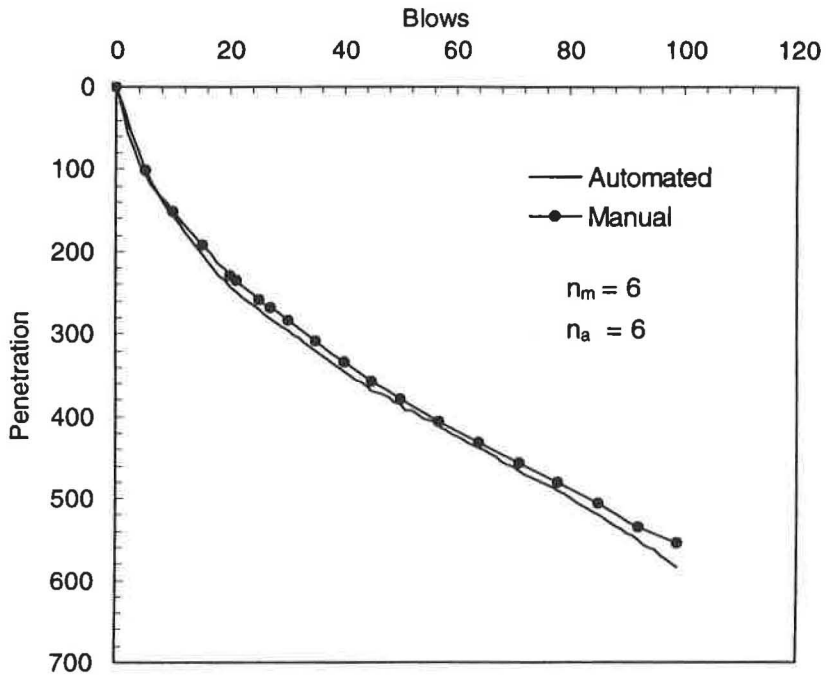

Figure 16. Comparison of Automated Manual DCP Penetration Resistance in A-2-4 Soil

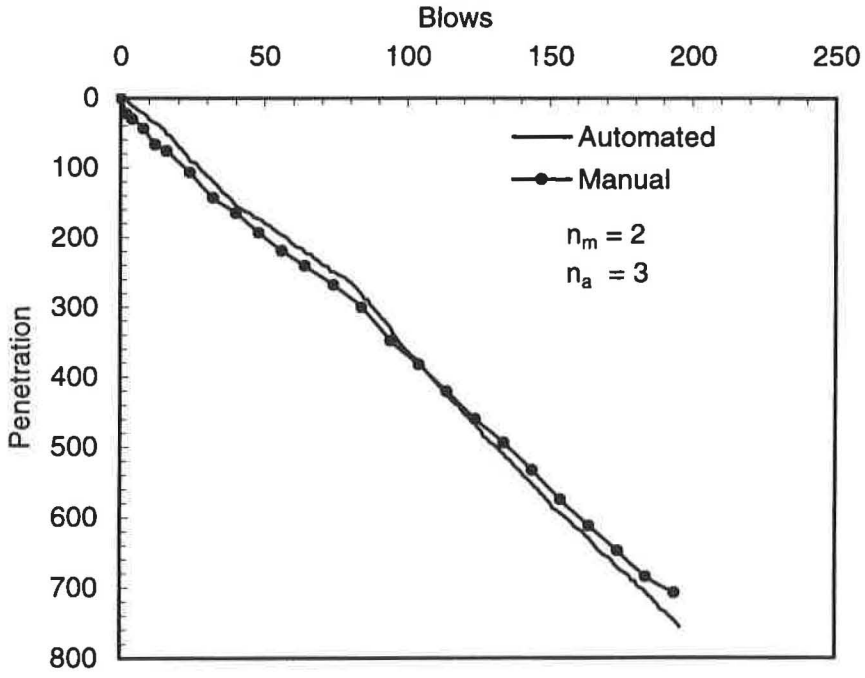

Figure 17. Comparison of Automated and Manual DCP Penetration Resistance in Limerock Base and Stabilized Subgrade, Test Pit Series 2, Center Section

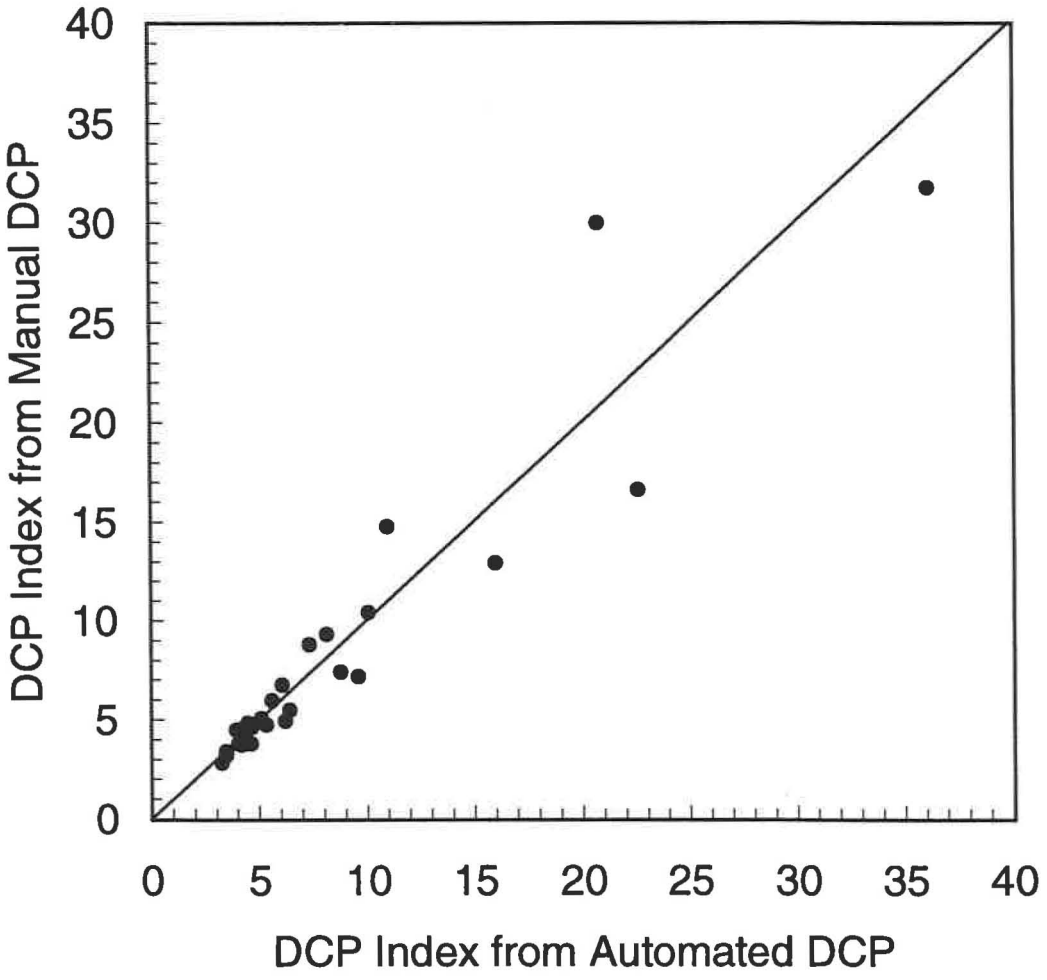

Figure 18. Comparison of DCPI from Automated and Manual DCP

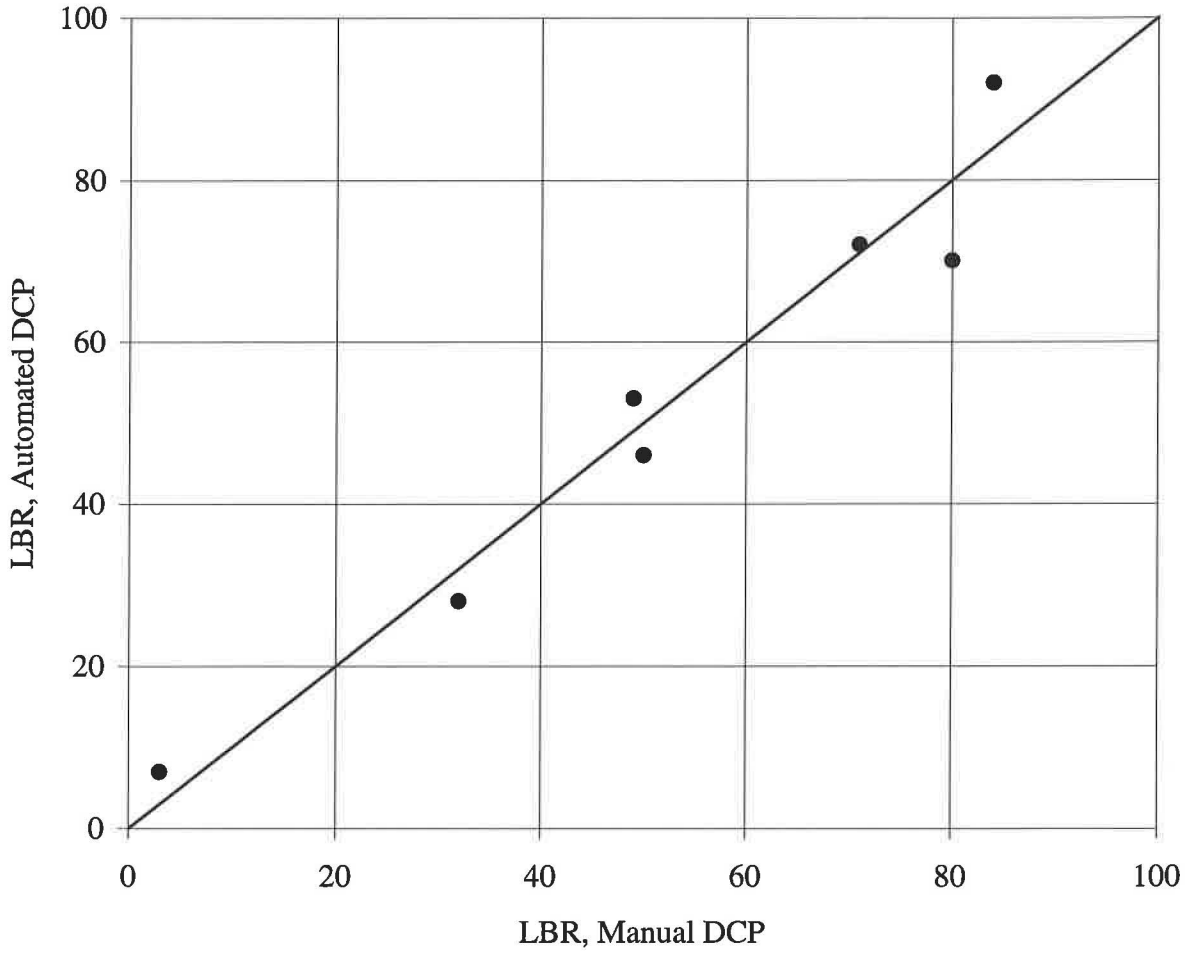

Figure 19. Comparison of Average LBR Computed with Manual and Automated DCPI

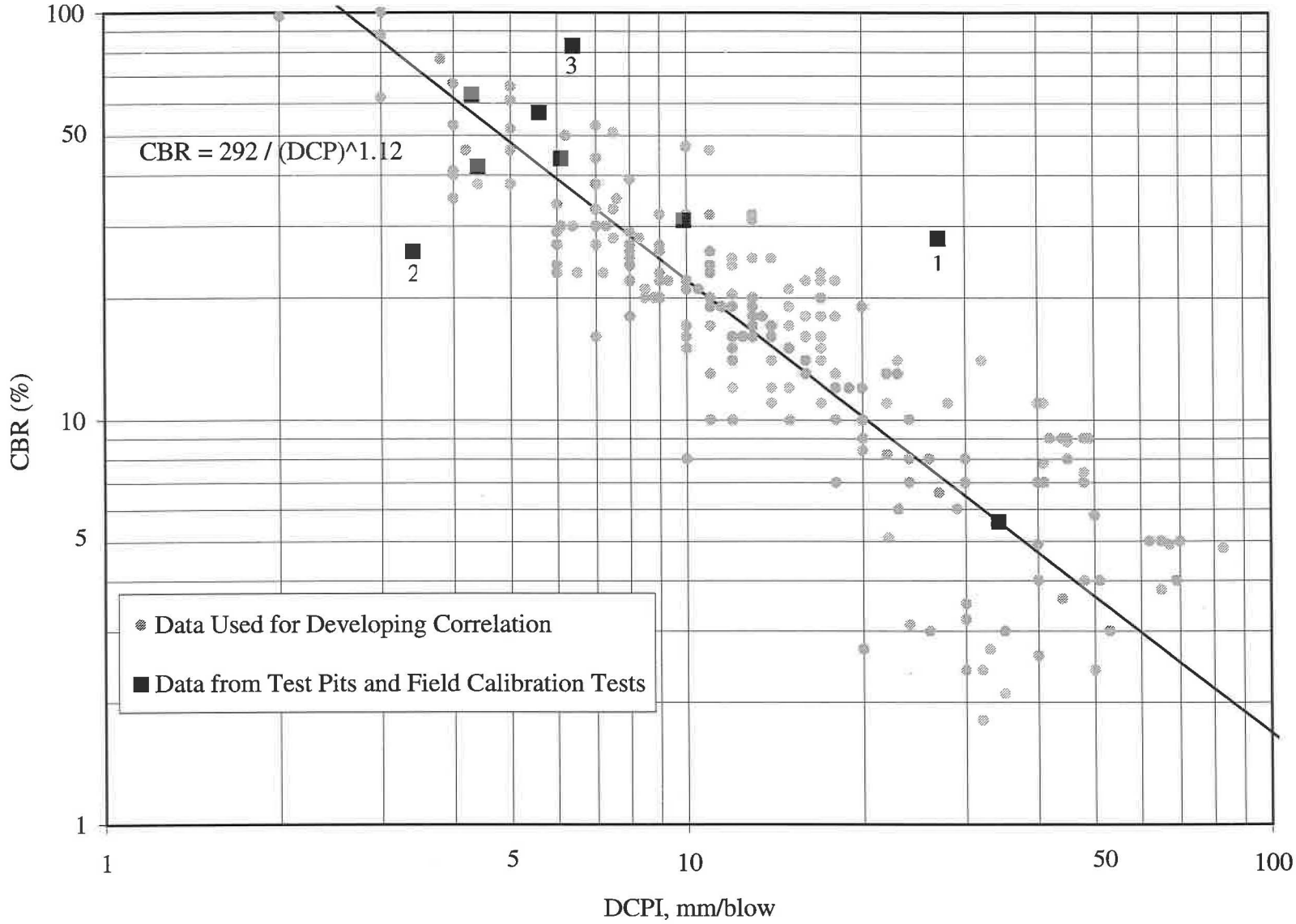

Figure 20. Comparison of Data for Florida Soils and Paving Materials with CBR/DCPI Correlation

The numbered points (1-3) indicate some lack of fit, but may be explainable. Point 1 is for the I-75, A-3 Sand Subgrade Section. The sand was very fine and saturated when tested. Driving the cone penetrometer may have produced excess pore pressures resulting in decreased effective stress and consequently reduced strength. This could explain the indicated nonconformance with measured CBR/LBR where the loading is applied at the much slower rate.

Point 2 is for the limerock base in Test Pit, Series 2, Center Section. The DCPI indicates higher values than the measured 26CBR/32LBR. The exact reason for this is not known, but the measured CBR/LBR's at testing and during construction were atypically low for limerock base and much lower than obtained in the laboratory, see Table 2.

Point 3 is for the A-2-4 clayey sand in Test Pit Series 1, Center Section. The DCPI indicates lower values than the measured 83CBR/104LBR. Again, the cause is speculative, but in this case the measured CBR/LBR at testing was atypically high for A-2-4 soil. It was also higher than laboratory or as constructed CBR/LBR values, see Table 2. The nonconformance may be due to significant drying between the time the ADCP tests were run and the time trenching and CBR/LBR testing was conducted.

Reduced Hammer Drop Height

The dual mass DCP, Figure 1, has a full drop height of 575 mm (22.6 in.). When used in the Florida DOT ADCP, the DCP is mounted in a carriage for controlling cone penetration. With softer soils, the full drop height may cause the anvil to "bottom out" by impacting the bottom of the carriage. This will occur when the penetration for a blow exceeds the clearance between the bottom of the anvil and the bottom of the carriage. The maximum clearance when the carriage is adjusted downward is adjusted downward is 75 mm (3 in.) and decreases as blows are applied until another adjustment is made. The 75 mm (3 in.) clearance corresponds to the penetration that might be achieved with one blow in soil with LBR of about 3.

To reduce cone penetration to levels that are manageable with the control mechanisms on

the ADCP, either the hammer weight or drop height can be reduced. The most effective option is reduced drop height which can be controlled with the ADCP operation software.

Limited trials with variable drop height were conducted in the test pit studies. The results of half and quarter drop height trials are shown in Figures 21 and 22. Ratios of DCPI for half and quarter drop heights to DCPI for full drop height are plotted versus penetration. Although additional testing is needed to improve confidence, the mean ratios of 0.6 and 0.3 are suggested for modifying DCPI measured with half and quarter drop heights, respectively. The modified DCPI's are appropriate for estimating LBR's with Equation 11.

The mean ratios of 0.6 and 0.3 represent real systems and appear realistic based on theoretical energy and momentum considerations for ideal systems. Potential energy of a mass (m) at a height (h) is

$$PE = mgh \quad \ldots\ldots (12)$$

Where g = acceleration due to gravity. This potential energy is converted to kinetic energy when the mass free falls. Kinetic energy is computed as

$$KE = \tfrac{1}{2} mv^2 \quad \ldots\ldots (13)$$

where, for ideal systems

v = mass velocity.

$$= (2gh)^{1/2} \quad \ldots\ldots (14)$$

Linear momentum of a free falling mass is computed as

$$G = mv \quad \ldots\ldots (15)$$

Based on energy considerations, drop height reductions of a half and a quarter would reduce potential and, therefore, kinetic energy at impact to 50 and 25% of full drop height values. The

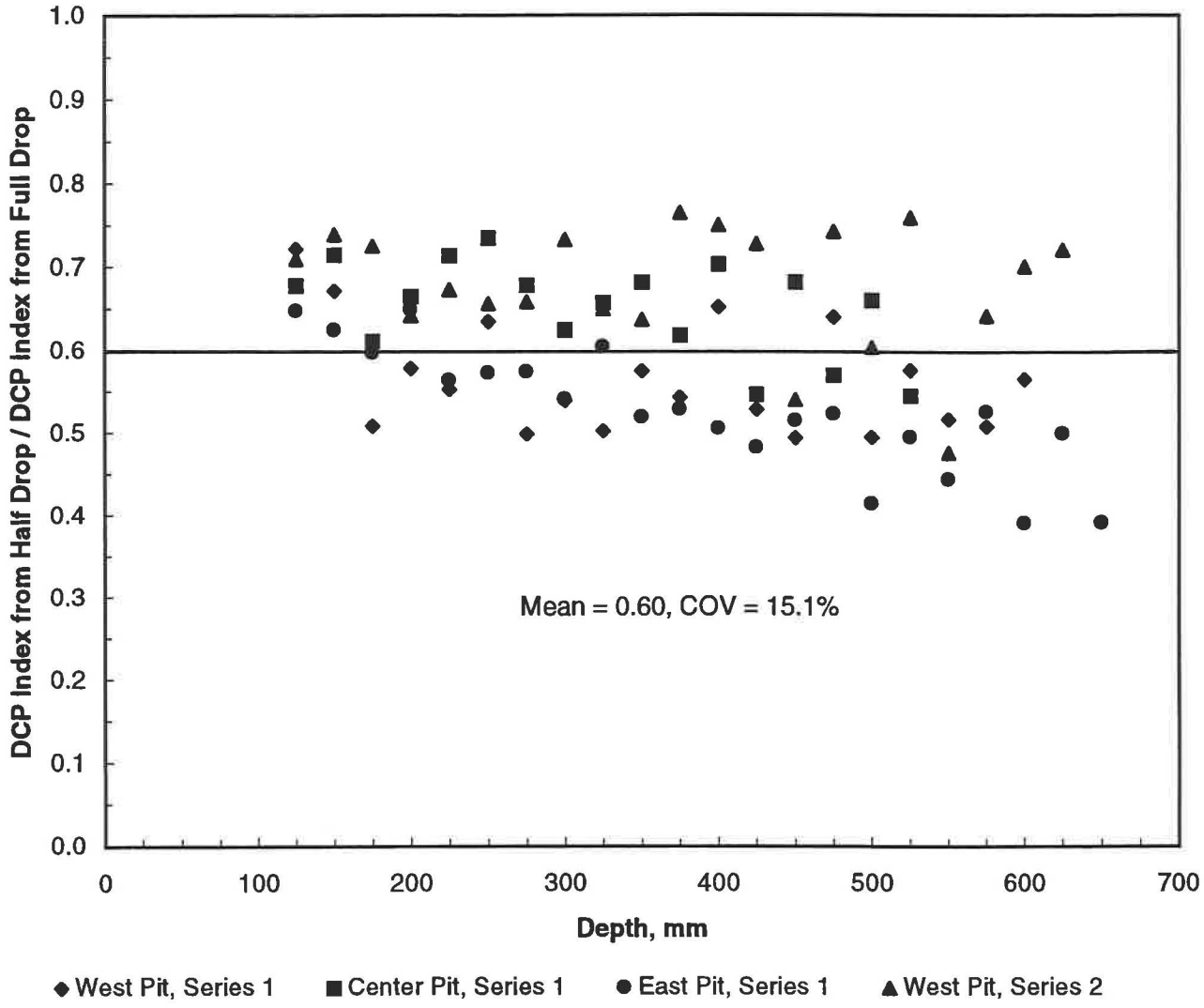

Figure 21. Comparison of DCPI for Full and Half Drop Heights.

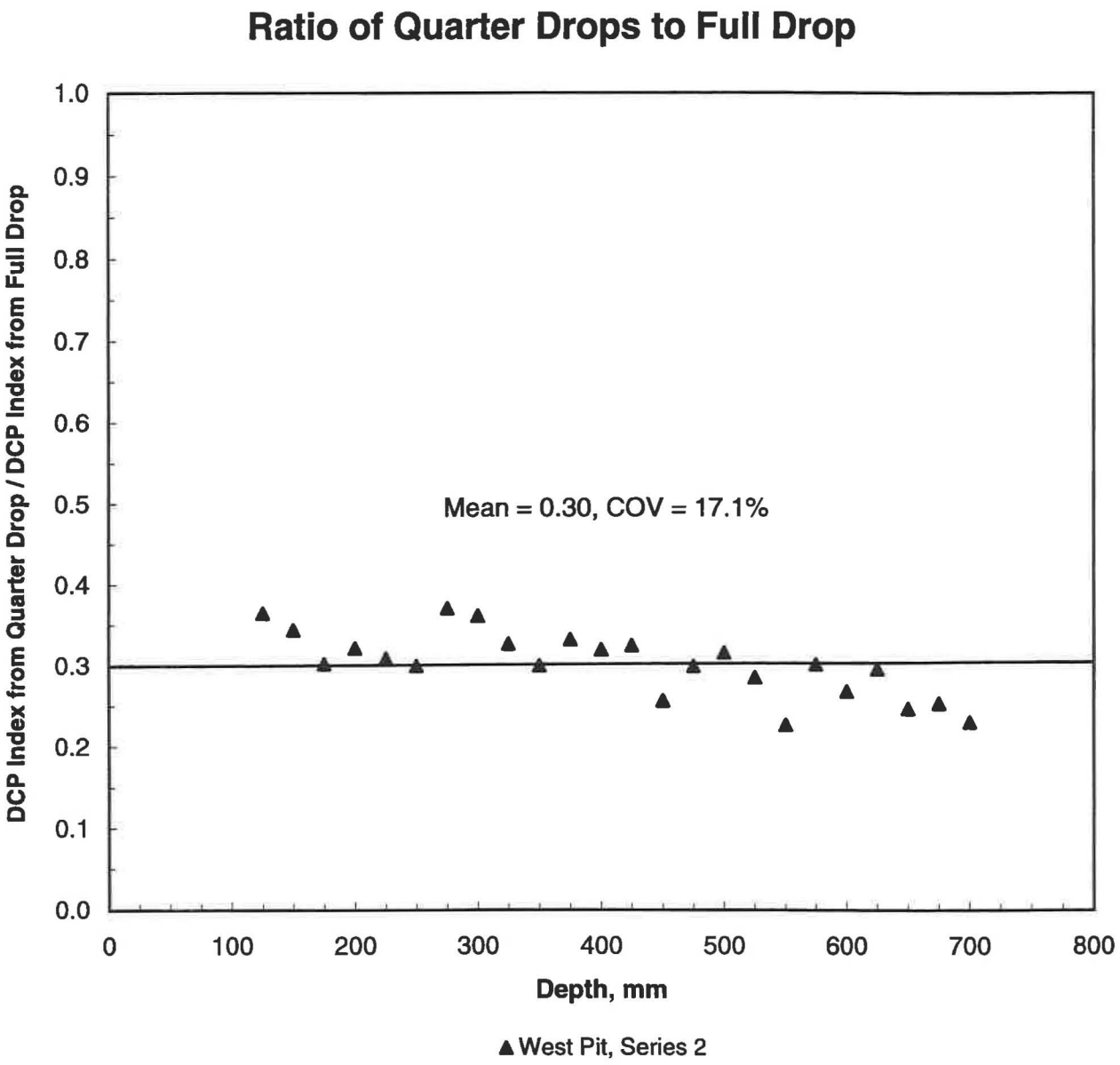

Figure 22. Comparison of DCPI for Full and Quarter Drop Heights.

measured ratios of 0.6 and 0.3 are both somewhat higher and suggest that more energy is lost for full height drops than for partial height drops.

Velocity at impact for half and quarter height drops, relative to velocity for full height drops, are

$$v_{1/2} = \frac{v}{\sqrt{2}} \quad \text{(16)}$$

and

$$v_{1/4} = \frac{v}{2} \quad \text{(17)}$$

This means the corresponding ratios of linear momentum transferred to the anvil at impact relative to that transferred for full height drops are $\frac{1}{\sqrt{2}} = 0.71$ and ½ = 0.5, respectively. Contrary to energy comparisons, these ratios are somewhat larger than the measured DCPI ratios of 0.6 and 0.3.

Effects of Confinement

Confinement from overlying layers increases soil and paving material strength. In laboratory LBR tests the effects of confinement are simulated by surcharge weights placed on samples. This approach was tried on a limited basis for I-75 sections and Test Pit, Series 2 tests. Data from these tests are tabulated in Table 5 and plotted in Figure 23. Figure 23 shows there was no apparent effect of vertical pressure, up to 0.84 psi, from the 1 or 2 ft. dia. steel plates.

A 5 in. limerock base layer was constructed on the A-1-b sand in the West Section of Test Pit Series 2. The ADCP cone was driven through the limerock base and into the sand. Figure 24 is a plot of LBR versus penetration with and without the limerock base layer that demonstrates it's strengthening effect. This is due directly to confinement during ADCP testing as well as some additional compaction in the sand layer as the limerock base layer was placed and compacted. The confinement provided by the limerock base layer would have greatly enhanced the effectiveness of additional compaction energy transmitted to the sand.

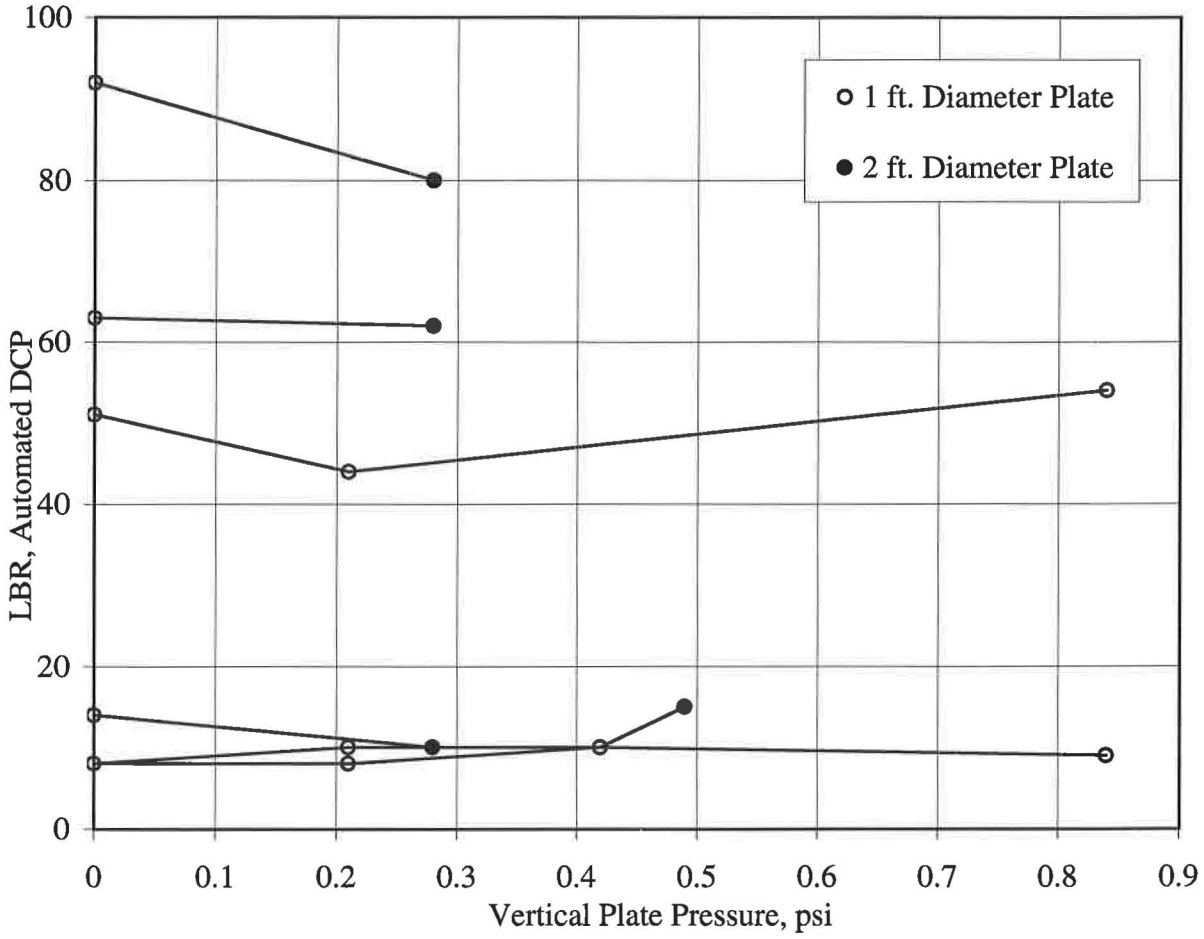

Figure 23. Effects of Vertical Plate Pressure on LBR Measured with DCPI

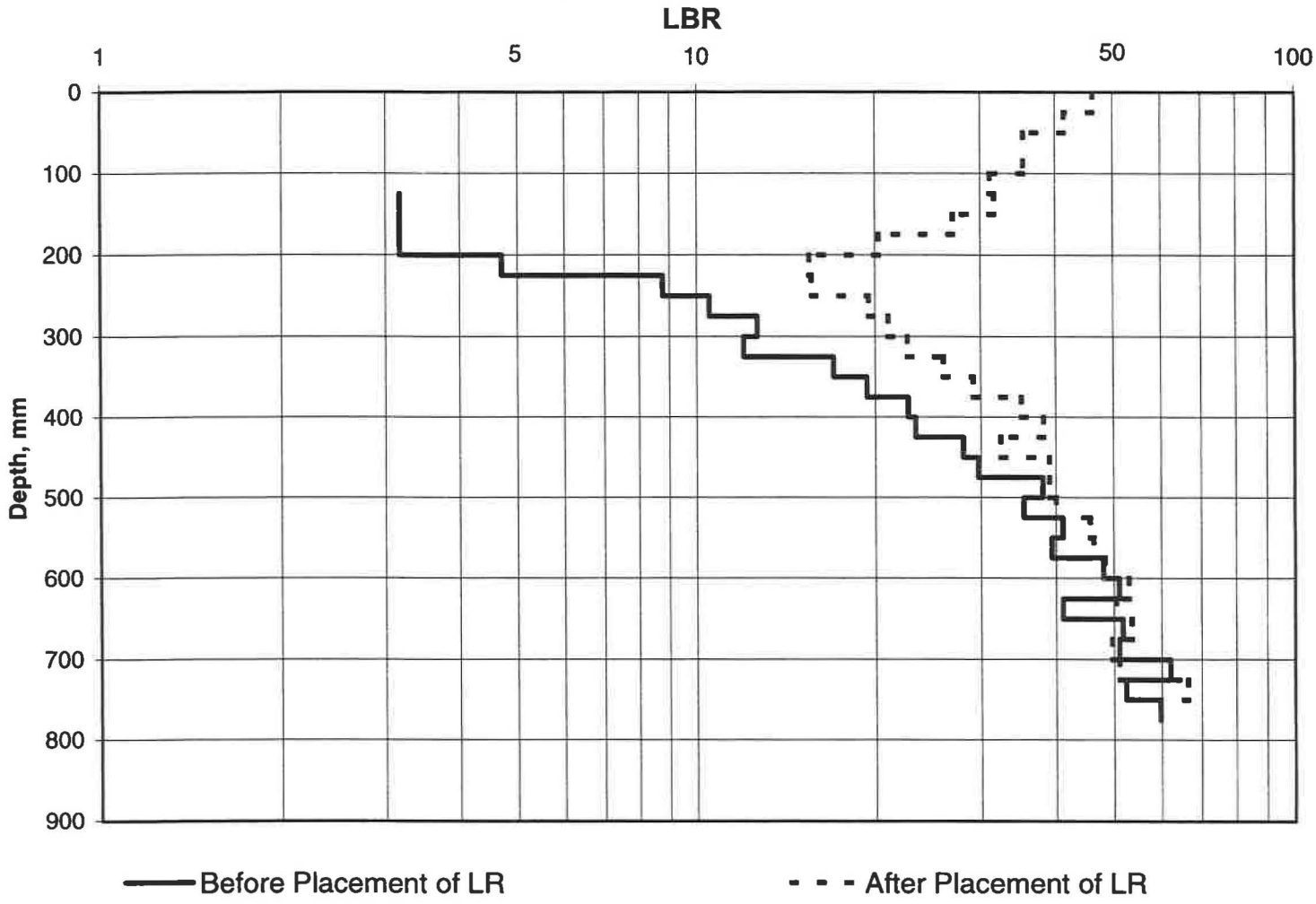

Figure 24. Effects of Limerock Base Layer on Strength of A-1-b Sand

Based on a limerock density of 120 lb/ft^3, the vertical pressure from the 5 in. layer was approximately 0.35 psi. The average LBR = 25, shown in Table 5, is obviously larger than values for comparable plate pressures. Based on these limited trials, it is concluded that the confining effects of overlying layers cannot be practically simulated with metal plates.

Webster, Brown and Porter (12) tried a somewhat different approach. They developed data for determining DCP penetration in various types of soil where predicted CBR's matched measured values at the soil surface. Uniform soil layers were constructed and CBR tests run on the surfaces. DCP tests were run and CBR's with depth estimated from DCPI's. Depths determined where CBR's matched CBR's measured at the surface are tabulated in Table 6. The depths are small for soils with strength due primarily to cohesion and increase for soils with strength due primarily to friction.

Table 6. DCP Depth Required to Measure Surface Layer Strength, No Overburden (after Webster, Brown and Porter (12))

Test Location	Soil Type	Average Penetration Depth Required, in.
WES	CH	1
WES	CL	3
WES	SC	4
WES	SW-SM	4
WES	SM	5
WES	GP	5
WES	SP	11

Effects of Moisture and Density

Density and water content affect soil and paving material strength. For strictly cohesionless soils and paving materials, density is the dominant influence. But for most soils, which have some cohesive component, both water content and density affect strength. Classical

relationships are shown in Figure 25 (14). Figure 25 indicates there may be significant differences between samples compacted to the same density but at different water contents, and samples compacted to the same water content and density but tested as compacted or saturated. The data in Table 2 for the test pits also illustrates these differences.

Implications of the effects of density and moisture is that a procedure relating field LBR with laboratory/design LBR is required to set acceptance criteria, if the ADCP is to be used for construction quality control/assurance (QC/QA). More specifically, a procedure is required to account for the influence of low water content; low density effects will be correctly reflected in measured DCPI.

No tests were run as part of this study to develop required relationships. However, a methodology based on laboratory tests is offered for consideration.

When developing compaction curves for soil or paving materials, two samples should be compacted at each water content. A soaked (standard procedure) and unsoaked LBR test should be conducted on these samples. From the data thus obtained, usual compaction curves for selecting required field water content and dry density may be selected. In addition, a procedure for setting required field LBR for acceptance, illustrated in Figure 26, can be developed. Soaked and unsoaked LBR are plotted versus as compacted water contents. The difference between the two curves should approximate the difference between as constructed field conditions and design conditions.

The proposed procedure will require water content measurements as ADCP tests are conducted. The LBR adjustment, Δ_{LBR}, is selected at the field water content as illustrated in Figure 26. This LBR adjustment is added to the design LBR to obtain the minimum field LBR for

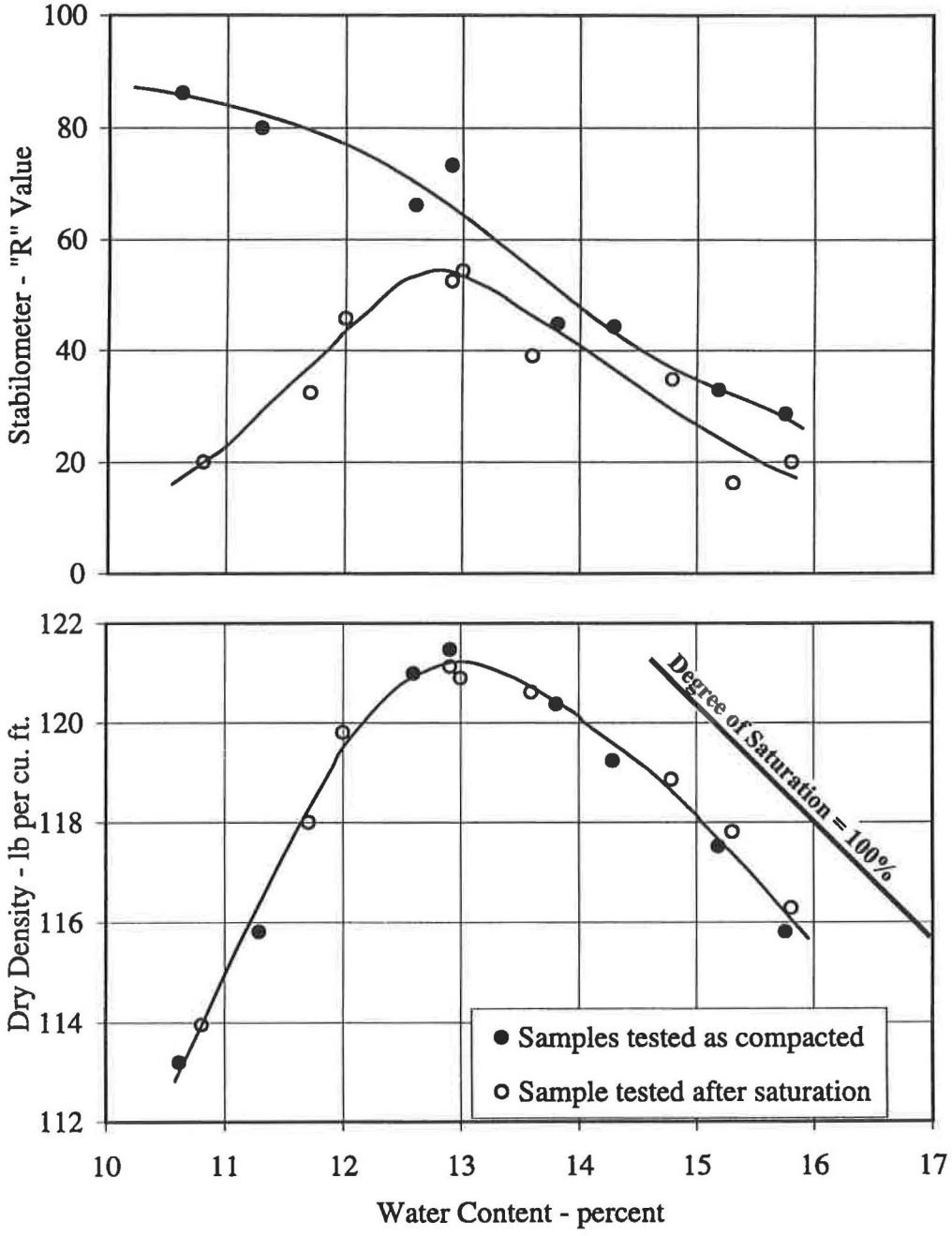

Figure 25. Effect of Saturation on Stability of Compacted Samples of Sandy Clay (after Seed (14))

acceptance only when the field water content is less than the optimum water content.

$$LBR_{ADCP} \geq LBR_{Design} + \Delta_{LBR} \quad (18)$$

To efficiently achieve proper compaction, the water content of soils and paving materials should be within a few percentage points of the optimum water content. Drying back from compaction water contents will increase strength of most soils and paving materials. This increase in strength will develop in paving layers if they are allowed to dry and will be reflected in LBR estimated with the ADCP. The proposed procedure for adjusting design LBR should somewhat compensate for this, but increases in strength due to drying may be larger than the differences between soaked and unsoaked samples. Therefore, a minimum water content at ADCP testing is proposed to prevent excessive dry back. A second practical reason for setting a minimum water content is so that it is within the range of laboratory water contents.

Although no specifics can be offered for selecting Δ_w, it is suggested that the minimum water content should be based on optimum water content as

$$W_{min} = W_{opt} - \Delta_w \quad (19)$$

where

W_{min} = minimum water content at ADCP testing

W_{opt} = optimum water content for soil or paving material tested

Δ_w = water content adjustment.

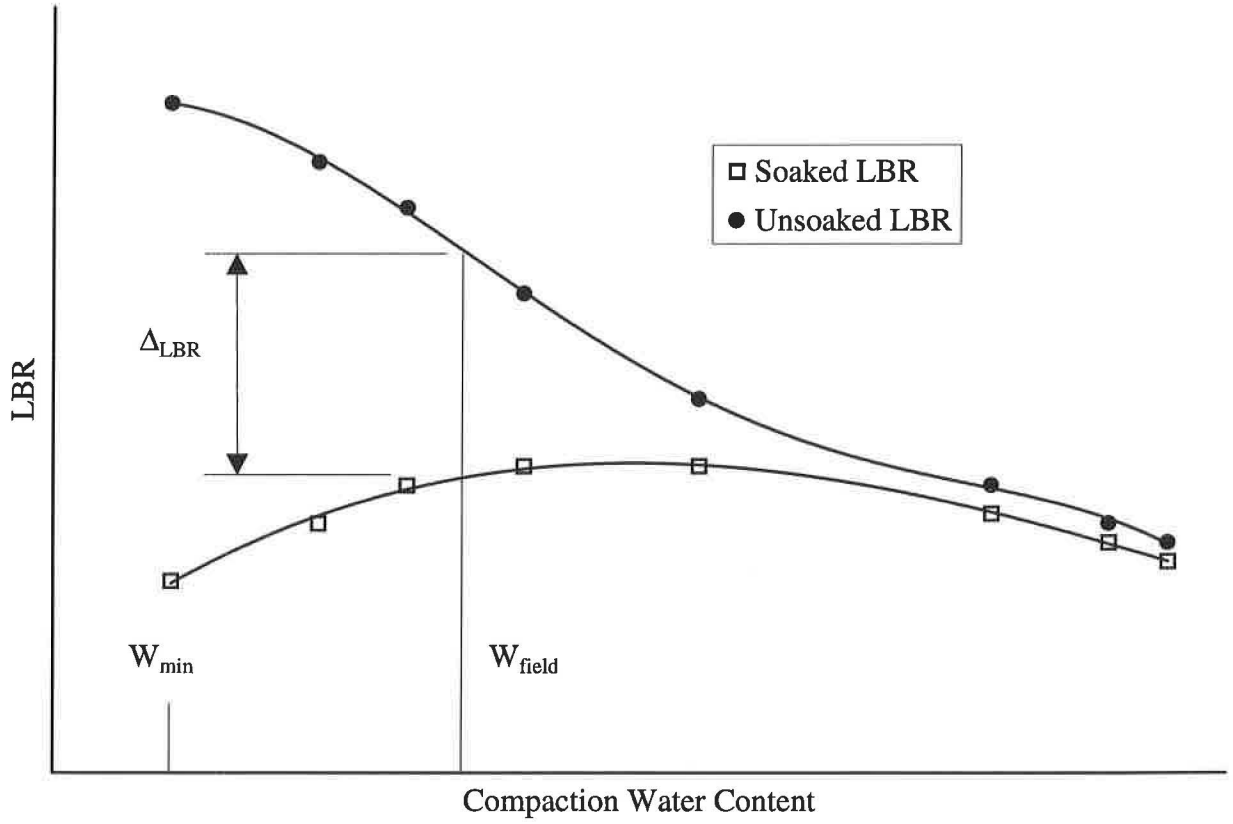

Figure 26. Adjustment of Field LBR for Saturation

CONCLUSIONS AND RECOMMENDATIONS

The Florida DOT ADCP provides a practical tool for measuring in situ strength of granular paving materials and soils. The correlation developed by Webster, Grau and Williams (5) is recommended for estimating CBR (LBR) with measured DCPI. For softer soils, half or quarter drop heights may be used and measured DCPI divided by 0.6 or 0.3, respectively to modify them for estimating CBR (LBR).

Evaluation of the strength of granular paving materials and subgrade soils in existing pavements is readily accomplished with the Florida DOT ADCP, requiring only access through bound layers. Strength parameters estimated with measured DCPI will accurately reflect actual conditions within pavement structures.

Additional research will be required in order to effectively utilize the ADCP for construction control. Relationships are needed between laboratory/design strength parameters and field strength parameters in order to set acceptance criteria. In particular, differences in confinement, moisture content, and density must be considered. For satisfactorily constructed paving layers, design conditions may not be achieved for full depths. Criteria is needed to determine acceptable depths of noncompliance at the top and bottom of paving layers.

REFERENCES

1. Fenwick, W. B., "Description and Application of Airfield Cone Penetrometer", Instruction Report No. 7, US Army Engineer Waterways Experiment Station, Vicksburg, MS, October 1965.

2. Croney, P. and D. Croney, The Design and Performance of Road Pavements, Third Edition, McGraw-Hill, New York, 1997.

3. Van Vuuren, D. J., "Rapid Determination of CBR with the Portable Dynamic Cone Penetrometer", The Rhodesian Engineer, Vol. 7, No. 5, September 1969.

4. Kleyn, E. G., "The Use of the Dynamic Cone Penetrometer", Transvaal Roads Department, South Africa, July 1975.

5. Webster, S. L., R. H. Grau and T. P. Williams, "Description and Application of Dual mass Dynamic Cone Penetrometer", Instruction Report GL-92-3, US Army Engineer Waterways Experiment Station, Vicksburg, MS, May 1992.

6. Livneh, M., I. Ishai and N. A. Livneh, "Carrying Capacity of Unsurfaced Runways for Low Volume Aircraft Traffic", Air Force Engineering and Service Center, Tyndall Air Force Base, FL, February 1992.

7. Ese, D., J. Myre, P. Noss and E. Vaerness, "The Use of Dynamic Cone Penetrometer (DCP) for Road Strengthening Design in Norway", Proceedings, Fourth International Conference on Bearing Capacity of Roads and Airfields, Minneapolis MN, July 1994.

8. Smith, R. B. and D. N. Pratt, "A Field Study of In Situ California Bearing Ratio and Dynamic Cone Penetrometer Testing for Road Subgrade Investigations", Australian Road Research Board 13 (4), December 1983.

9. Hasim, M. S. B., M. S. B. Mustafa and Z. A. B. M. Kasim, "Quick-Insitu-CBR for Road Engineering from DCP/Insitu-CBR Relationship Developed in Malaysia", (unknown origin and date).

10. Livneh, M. "The Use of Dynamic Cone Penetrometer in Determining the Strength of Existing Pavements and Subgrades", Proceedings, Southeast Asian Geotechnical Conference, Bankok, Thailand, 1987.

11. Harison, J. A., "In Situ CBR Determination by DCP Testing Using a Laboratory-Based Correlation", Australian Road Research, Technical Note No. 2, December 1989.

12. Webster, S. L., R. W. Brown and J. R. Porter, "Force Projection Site Evaluation Using the Electric Cone Penetrometer (ECP) and the Dynamic Cone Penetrometer (DCP)", Technical Report GL-94-17, US Army Engineers Waterways Experiment Station, Vicksburg, MS, April 1994.

13. "AASHTO Guide for Design of Pavement Structures", American Association of State Highways and Transportation Officials, Washington, DC, 1993.

14. Seed, H. B., "A Modern Approach to Soil Compaction", Proceedings, Eleventh California Street and Highway Conference, Reprint No. 69, The Institute of Transportation and Traffic Engineering, University of California at Berkeley, 1959.